A Comprehensive Review on the Characteristics and Modeling of Lithium-Ion Battery Aging

Vermeer, Wiljan; Mouli, Gautham Ram Chandra; Bauer, Pavol

DOI
10.1109/TTE.2021.3138357

Publication date
2022

Document Version
Accepted author manuscript

Published in
IEEE Transactions on Transportation Electrification

This article has been accepted for publication in a future issue of this journal, but has not been fully edited. Content may change prior to final publication. Citation information: DOI 10.1109/TTE.2021.3138357, IEEE Transactions on Transportation Electrification

A Comprehensive Review on the Characteristics and Modelling of Lithium-ion Battery Ageing

Wiljan Vermeer, *Student Member, IEEE,* Gautham Ram Chandra Mouli, *Member, IEEE,* Pavol Bauer *Senior Member, IEEE*

***Abstract*—Battery ageing is one of the critical problems to be tackled in battery research, as it limits the power and energy capacity during the battery's life. Therefore, optimizing the design of battery systems requires a good understanding of ageing behaviour. Due to their simplicity, empirical and semi-empirical models are frequently used in smart charging studies, feasibility studies, cost analyses studies, among other uses. Unfortunately, these models are prone to significant estimation errors without appropriate knowledge of their inherent limitations and the interdependency between stress factors. This paper presents a review of empirical and semi-empirical modelling techniques and ageing studies, focusing on the trends observed between different studies and highlighting the limitations and challenges of the various models. First, we summarize the main ageing mechanisms in lithium-ion batteries. Next, empirical modelling techniques are reviewed, followed by the current challenges and future trends, and conclusion. Our results indicate that the effect of stress factors are easily oversimplified, and their correlations often not taken into account. The provided knowledge in this paper can be used to evaluate the limitations of ageing models and improve their accuracy for various applications.**

***Index Terms*—Lithium, battery, degradation, ageing, modelling.**

I. Introduction

SINCE they were first commercialized by Sony in 1991 [1], lithium-ion battery (LIB) technology has been widely adopted due to its relatively high energy and power density, high efficiency, and rather long lifetime [2]. Today LIBs play a vital role in the energy transition; they help integrate renewable energy sources (RES), provide ancillary services, and reduce transportation emissions. Additionally, LIBs are also widely used in the mobile device industry, aerospace & aviation industry, and defence industry [3], [4]. All of this contributes to a rapidly increasing LIB market. However, despite its growing market and relatively good performance, climate change, and particularly electric vehicle (EV) applications, push for lower costs and higher energy densities over a long lifetime. Unfortunately, these metrics are generally trade-offs, and therefore understanding battery ageing and modelling is critical for optimizing LIB performance.

This paper presents a review of empirical and semi-empirical modelling techniques and ageing studies, focusing on the trends observed between different studies and highlighting the limitations and challenges of the various models.

The authors are with the department DC Systems, Energy Conversion & Systems, Technical University, Delft 2628, The Netherlands.

J. Doe and J. Doe are with Anonymous University.

Manuscript received April 19, 2005; revised August 26, 2015.

A. Battery Ageing Modelling

Methods for modelling LIB degradation behaviour are divided into four different categories: 1. Physics-Based Models (PBM), 2. Equivalent Circuit Models (ECM), 3. Machine Learning Models (MLM), and 4. Empirical and semi-empirical Models (EM). A comparison of these models is given in Table I. Physics-based models, also known as electrochemical models intend to model the electrochemical and physical processes in the battery. The first PBM was developed by Doyle and was based on the porous electrode model [5], [6]. The psuedo-2D model expanded on this by adding a thermal model [7], including diffusion kinetics and Butler-Volmer kinetics [6]. Later, the effect of parasitic side reactions, such as solvent oxidation [8] or SEI layer growth [9], [10] were added to these equations to account for degradation. Others have tried to reduce the computational complexity for these models to be more widely applicable [11]. PBMs can achieve high accuracy, but they require many partial differential equations and a thorough understanding of all physical and chemical mechanisms. Furthermore, LIB ageing is frequently caused by multiple factors, making molecular modelling even more difficult and prone to miss out on macro-level effects [12]. As a result, electrochemical models are generally not used by non-chemical engineers/researchers [13].

Equivalent circuit models (ECM) do not require this information and instead model the transient response of the battery using passive circuit components such as resistances, capacitances, and inductances. More complex models can also be used to simulate the internal diffusion and charge transfer processes. And based on impedance data, ageing can be incorporated using variable components. This, however, requires large test matrices to quantify the ageing with respect to operational conditions. Due to their mathematical simplicity, they are frequently used in real-time applications, such as battery state estimations [14]. Often combined with state-estimators such as Kalman- or particle filters [12], [14].

Another common state-of-charge (SoC) and state-of-health (SoH) estimation technique involves machine learning (ML), such as support vector machine or neural networks. Different

TABLE I: Comparison of different ageing model techniques.

Model	Complexity	Accuracy	Amount of data	Applications
PBM	high	high	low	battery design
ECM	medium	medium	high	SoH estimation
MLM	medium-high	medium	high	SoH estimation
EM	low	low-medium	high	System design & Optimization

ML approaches exist, some train the algorithm to extract the SoH from the differential voltage curve or incremental capacity curve of the battery [15], [16]. The advantage of these approaches is that they only require easily obtained parameters such as voltage, current and temperature. Others combine ML with different models to train the algorithm based on model parameters such as ohmic resistance, polarization resistance and polarization capacitance [17], [18], or combine empirical modelling techniques with regression models to predict the SoH [19]. High accuracies can be obtained with ML methods, however, large data sets are needed to train the algorithms [12], [20]. Finally, empirical and semi-empirical models (abbreviated as EM) curve-fit the relationship of various stress factors onto the data resulting in a relatively simple analytical formula. Their simplicity allows using EMs in a wide variety of studies, such as system-level design problems, optimization models, battery management systems, among other things. Additionally, the analytical formulae give an intuitive feel to the effect of various stress factors. However, large test matrices are required to decouple their impact (if even possible), which is generally limited by the available equipment. As a result, EMs are prone to oversimplify the complex behaviour of LIB ageing and the correlation between stress factors, this is discussed in more detail in the next section.

B. Challenges of Empirical and Semi-empirical Ageing Models

Without a good understanding of LIB ageing behaviour and modelling limitations, the simplicity of EMs can pose challenges as they can easily lead to significant modelling errors. A summary of these challenges is given below:

1) Accelerated test conditions: ageing tests are frequently performed under accelerated ageing conditions such as high temperature, high C-rates, and high voltages to speed up ageing. While this reduces the amount of time required for testing, it also reduces the accuracy of the models when they are utilized outside of the test conditions. For example, models are often developed based on temperatures of 40°C and higher. Whereas very rarely models are tested below 25°C, and even fewer studies have evaluated multiple operating conditions below 25°C. As will be demonstrated in this study in section III.4, the use of testing conditions at temperatures that will never actually be reached or sustained for longer periods of time during normal operation can cause unreliable results. Especially at temperatures below room temperatures, where the effect of high-temperature ageing mechanisms will decrease, and other ageing mechanisms take over.
2) Limited test conditions: large test matrices are required to accurately model the effect of multiple stress factors, which are generally limited by the amount of available equipment. Here a good understanding of the expected ageing behaviour can help to determine the test conditions more strategically.
3) Stress factor interdependency: a good understanding of the interdependencies between stress factors is required to select an appropriate model and testing conditions for a particular use case. For example, based on the reviewed studies in this paper, it is observed that a strong correlation between the effect of temperature and C-rate exist. However, not many models model the interdependency of these stress factors. As a result, the actual operating range of the model might be limited to only the accelerated testing conditions. Furthermore, even within the test condition range, significant errors might occur when these interdependencies are not considered.
4) Modelling limitations: besides the effect of operational conditions, a good understanding of the model's fundamental limitations is also required. For example, depending on the chosen parametrical fit, EMs might be limited to a specific part of the battery lifetime or might be less suited for applications with very irregular charge cycles or applications with a different calendar- to cyclic ageing ratio.

The goal of this paper is to mitigate the effects of the above mentioned challenges and limitations by providing a comprehensive review of empirical and semi-empirical LIB ageing models, as well as the accompanied ageing behaviour.

C. Related Work & Scientific gap

In [21], [22] an in-depth review of the main ageing mechanisms on a material level is discussed. These studies are elaborated in [23], [24], where the authors also review the factors influencing ageing on a cell and battery pack level. The authors of [6], [12], [25] review the main ageing mechanisms and provide an overview of different ageing estimation techniques, including electrochemical models, equivalent circuit models, empirical models and statistical models. A similar approach for data-driven health diagnostics and prognostic techniques is performed in [20]. In [26] a comparison of several EMs is performed based on a conceptual smart grid framework. Furthermore, several studies have reviewed the various techniques for state-of-health estimation [27]–[30]. In [29] the authors discuss different types of self-adaptive SOH monitoring techniques, such as support vector regression, neural networks, or particle filter method. Additionally, a more broad overview of different types of SOH and remaining-useful-life (RUL) estimation techniques is given in [27], [28], [30], including direct measurement techniques, model-based techniques, and adaptive filtering techniques.

All of the papers mentioned above aim at providing a broad overview of different kinds of ageing mechanisms or ageing estimation techniques, whether that includes model-based techniques, data-driven techniques are self-adaptive techniques. In most of them, EMs are briefly mentioned as a part of this. However, given the scope of these papers, they do not provide an in-depth review of different empirical models, nor do they provide any insights into the correlations found between different studies. Even [26], which is entirely focused on EMs, provides a simplified description of the effect of operational stress factors. Furthermore, none of the above mentioned papers actually review and compare the ageing behaviour of different ageing studies, which makes it even more difficult to provide generalizations in terms of impact of

operational conditions, or modelling accuracy. As explained above, this is especially problematic for EMs, since without a proper understanding of battery ageing, empirical ageing modelling, and its limitations and challenges, the simplicity of EMs can easily lead to significant modelling errors in a wide variety of studies.

D. Contribution

LIB degradation is an important factor for developing new LIBs and optimizing their techno-economic performance. In this regard, multiple studies have reviewed the various methodologies for ageing estimation. However, based on the aforementioned challenges and related work it is concluded that a significant scientific gap still exists. Since no study has yet thoroughly reviewed empirical and semi-empirical models and has investigated the correlations between different studies, to highlight the limitations of the models, and focus on the reasons for the observed trends and insights. Due to the simplicity and widespread use of EMs, this can potentially result in significant modelling errors. To this extent, the main contributions of this study are summarized as follows:

1) A comprehensive review of empirical and semi-empirical modelling techniques for LIB ageing, with a focus on operational stress factors and their interdependence, modelling techniques, limitations, and challenges, so that these models can be used accurately at the relevant operating conditions.
2) A detailed review of the ageing behaviour of various LIB cells, investigating the correlations between different ageing studies and examining the relationship with operating conditions, ageing mechanisms, and modelling techniques.

E. Organization

The remainder of this paper is organized as follows. Section II summarizes the main ageing mechanisms for LIBs. Next, the review of ageing behaviour and different modelling techniques is discussed in section III. Here, a distinction is made between calendar and cyclic ageing. The modelling techniques, limitations and challenges, and key insights are discussed per stress factor for both calendar and cyclic ageing. Therefore the structure of Section III is as follows:

A. Calendar/Cyclic ageing
  A.1. Stress Factor X
    A.1.a Modelling Techniques
    A.1.b Modelling Limitations & Challenges
    A.1.c Key Insights

Next the current challenges and future trends regarding LIB ageing and ageing modelling are described in section IV. Finally, the conclusion is presented Section V.

II. Main Ageing Mechanisms

Figure 1 shows a simplified representation of an electrochemical battery. The four main components of a LIB are the:

1) Anode, the most often used material is graphite [31]–[33], other common materials are lithium-titanate-oxide (LTO) or Silicon [34].
2) Cathode, which is made of a composition material that contains Lithium. Commonly used materials are Lithium Iron Phosphate (LFP), Lithium Nickel Manganese Cobalt Oxide (NMC), Lithium Manganese Oxide (LMO), and Lithium Nickel Cobalt Aluminium (NCA).
3) Electrolyte, a composition of lithium salts and organic solvents [26]. The electrolyte is mainly used to transfer ions between the cathode and the anode.
4) Separator, a porous plastic that separates the anode and cathode to prevent short-circuiting the electrodes.

During charging, Li-ions deintercalate[1] from the cathode, move through the electrolyte and separator before they intercalate at the anode. The resulting flow of ions creates an electrical current opposite to the flow of electrons, as shown in Figure 1. The degradation of LIBs occurs during both cycling and idle state and is caused by physical stress, and chemical side reactions [2], [23]. Additionally, many factors influence battery degradation, such as cell chemistry, cell design, pack design, and operating conditions. LIB ageing is commonly categorized into three different ageing modes [21], [23], [32], [36], [37]:

1) Loss of Lithium Inventory (LLI): represents the loss of active lithium ions that are no longer available for cycling. Causes for LLI can be parasitic side reactions such as, surface film formation, decomposition reactions, lithium plating, among other things. LLI is associated with capacity fade, i.e. the loss of effective mAh of the cell.
2) Loss of Active Material (LAM): represents the loss or structural degradation of the available anode or cathode material. Possible causes include electrode surface layer growth or cycling induced cracks/exfoliation. LAM can cause both power and capacity fade.
3) Conductivity Loss (CL): also known as contact loss [21], describes the degradation of electrical parts such as the current collector corrosion and binder decomposition.

A fourth addition could be the loss of electrolyte, which would lead to LAM and CL after a certain point and is therefore not separately mentioned. Even though differentiated into three categories, the degradation modes often interact, and a single degradation mechanism such as surface layer formation can trigger multiple degradation modes. A summary of

[1]Intercalation is the insertion of molecules into the electrodes

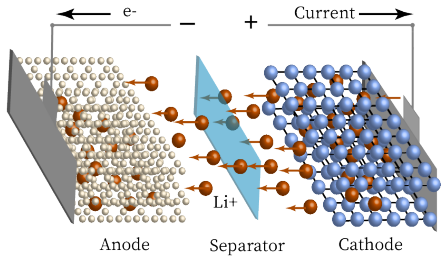

Fig. 1: A simplified representation of a lithium-ion battery consisting of an anode, cathode, separator, and electrolyte (the electrolyte is not shown for clarity, as it fills the entire battery). The arrows indicate a charging process where the Li-ions intercalate into the anode, resulting in an opposite electron flow.

operational conditions, the corresponding ageing mechanisms and their effect on LIB ageing is shown in Figure 2. Furthermore, A graphical representation of all ageing mechanisms is shown in Figure 3. The following two subsections will discuss these ageing mechanisms, here a division is made between the mechanisms that occur at the anode and the cathode, respectively. The ageing of the electrolyte and its effect on battery ageing mainly takes place at the electrodes [21] and is therefore not separately discussed.

A. Anode Ageing

The majority of LIBs use graphite as their anode material [21], [25], [38], so this section focuses on graphite based LIBs.

1) Solid Electrolyte Interphase Layer

The operating voltages of various common electrode materials in comparison to the electrochemical stability window of organic electrolytes are shown in Figure 4 . The operating voltage of graphite anodes is in the 0.05V-1V range [2], [39], which is outside the organic electrolyte stability window of 1V-4.5V. As a result, graphite-based LIBs are thermodynamically unstable, resulting in a reductive electrolyte decomposition reaction. This reaction consumes Li+ ions and forms a surface layer on the anode, resulting in LLI and LAM [2], [21], [33]. Especially in the first few cycles, the reaction rate is high, creating a surface layer permeable for Li-ions but less permeable for electrolyte components. This reduces the rate of decomposition and further electrode corrosion [21], [40]–[42]. However, even though the reaction rate reduces, the transport of solvated lithium and other electrolyte components through this semi-permeable layer continues throughout the battery's life. This reaction mainly occurs at the interphase between the electrolyte and the anode and is called the Solid Electrolyte Interphase (SEI) layer.

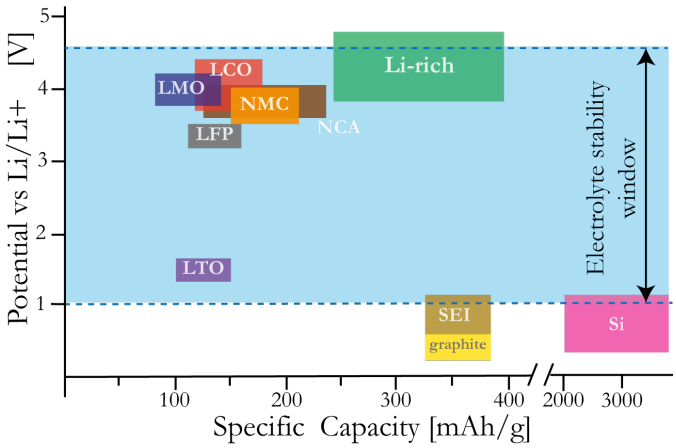

Fig. 4: Voltage versus energy capacity of five common electrode materials, compared to the electrochemical stability window of liquid organic electrolytes, adapted from [43], [44]. It shows that graphite is outside the electrochemical stability window of organic electrolytes, rendering graphite-based Li-ion batteries thermodynamically unstable and causing SEI layer growth.

The Solid Electrolyte interphase (SEI) layer's growth is often one of the main ageing factors of graphite anodes. It reduces the battery's available energy capacity and power handling capability. Another type of anode surface layer grows on the basal plane surface and is impermeable for Li-ions and therefore sometimes referred to as the non-SEI layer [45]. However, often the SEI and non-SEI layers are both referred to as SEI layer [21]. Therefore this convention is followed here as well.

After the initial formation of the SEI, it continues to grow during both cycling and idle conditions. The rate at which the SEI layer grows is dependent on the operating conditions

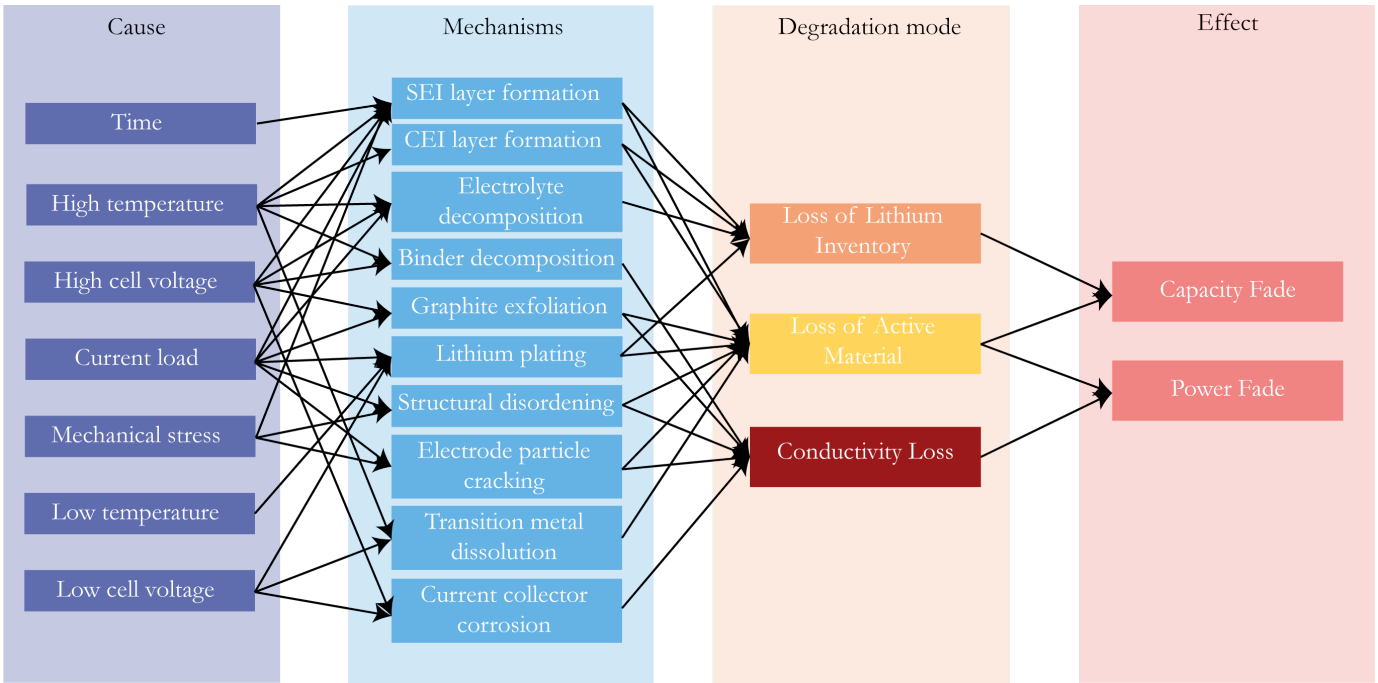

Fig. 2: Overview of the correlation between operational stress factors (the causes for degradation), the corresponding ageing mechanisms, ageing mode, and their effect on LIB ageing. Based on a combination of [2], [32], [35].

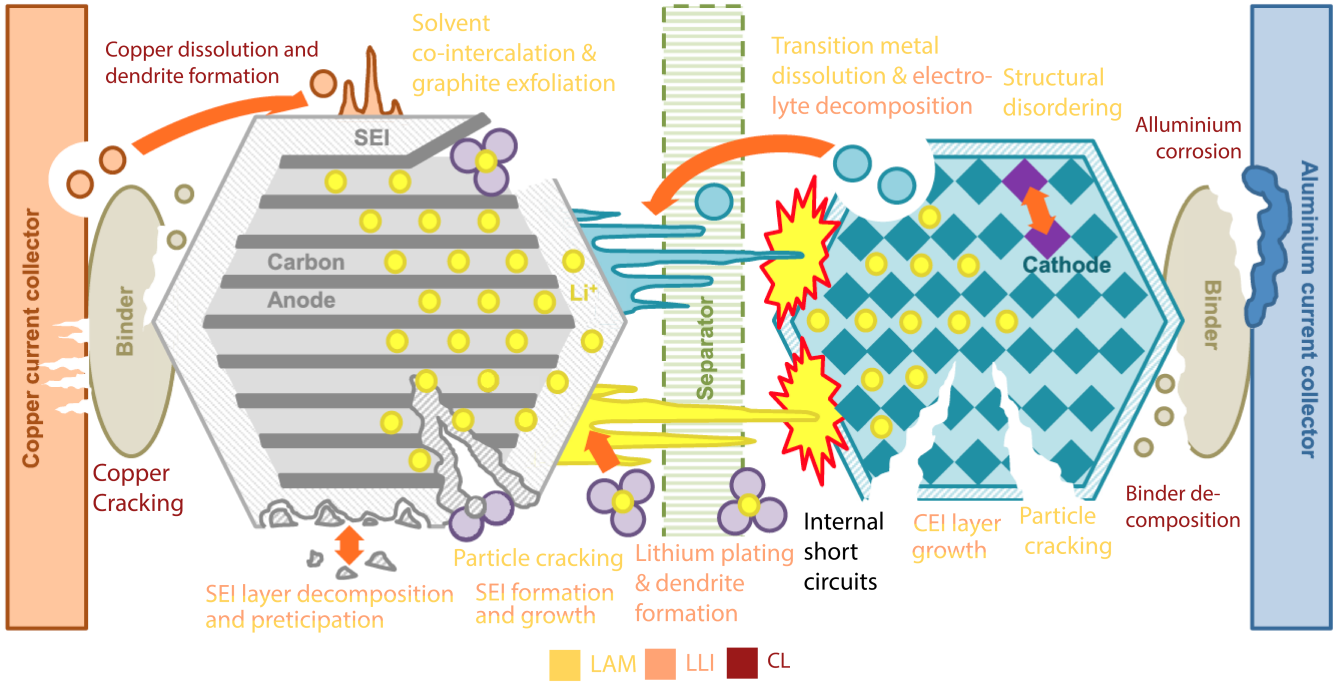

Fig. 3: Graphical summary of ageing mechanisms in graphite based LIBs. The ageing mechanisms are colour coded with respect to the accompanied degradation mode. The figure is adapted from material made publicly available by C.R. Birki et al. in [32], under Creative Commons Attribution 4.0 License CC-BY.

of the cell [46], [47]. During idle conditions, SEI growth is mainly driven by temperature and state of charge (SoC). At a higher SoC, more Li-ions are intercalated into the anode, decreasing the anode potential and increasing the reductive reaction rate [39]. Additionally, an increasing temperature also increases the reaction rate and might cause the less stable organic SEI components to change into more stable inorganic products, reducing the SEI layer's ionic conductivity. At extreme temperatures above 60°C even thermal runaway can cause the cell to catch fire or explode. from SoC and temperature, volume changes caused by the (de-)intercalation of Li-ions during cycling cause mechanical stress on the electrodes. These volume changes can crack the SEI, allowing new reactions to occur. As a result of this crack and repair, the SEI continues to grow, resulting in additional LLI and LAM [21], [48], [49]. Furthermore, cycling, especially with high C-rates, creates a more porous SEI layer compared to idle conditions [46], [47]. This increased porosity allows for more reductive reactions to occur, whereas a more dense SEI layer reduces the reaction rate. Other factors influencing the reaction rate are electrolyte composition and electrode balance [42], [50].

Two opposing theories exist regarding SEI formation: 1. The first theory assumes that the formation takes place at the electrode/electrolyte interface and that the electronic conductivity of the SEI should be the limiting factor of formation [51]. 2. The second theory states that SEI formation takes place at the anode-SEI interface and is limited by the solvent diffusion process [52]. However, both theories result in an ageing behaviour that follows a $\sqrt{\text{time}}$ relationship, which is typical for the passivation character of the SEI layer and similar to what is often observed in experiments.

2) Lithium plating

At lower temperatures, generally below 20°C, the diffusion rate of lithium into the anode or electrolyte reduces, and the intercalation potential of graphite material approaches that of metallic lithium. Metallic lithium plating may occur as a result of this. Lithium plating is especially likely to occur at low SoC, low temperature, and high C-rates [32]. Furthermore, after a certain age, the anode resistance can reach a critical limit. After this limit, the anode potential drops below 0V vs Li/Li+, and lithium plating starts to occur [47], [53].

Unlike SEI layer growth, lithium plating is a positive reinforcing phenomenon: as it occurs, it deposits on the anode, reducing the active surface area and resulting in a higher current density at the remaining available pores, further increasing the metal plating. As a result, a knee-point in the degradation behaviour is frequently observed at the age at which lithium plating occurs. An example of this is shown in Figures 5 (a)-(b), where two inflexion points are observed in both the capacity and impedance deterioration. Lithium plating causes LLI and possibly reduces the cell's safety, as lithium dendrites can start to grow, leading to internal short circuits [21].

3) Mechanical Stress at Anode

The intercalation of lithium ions into the anode can result in abrupt changes in volume as the particles undergo a phase transition [21], [54]. During a phase transition, the orientation of the molecules changes as more lithium is inserted, resulting in different geometrical and electrical properties. This causes

This article has been accepted for publication in a future issue of this journal, but has not been fully edited. Content may change prior to final publication. Citation information: DOI 10.1109/TTE.2021.3138357, IEEE Transactions on Transportation Electrification

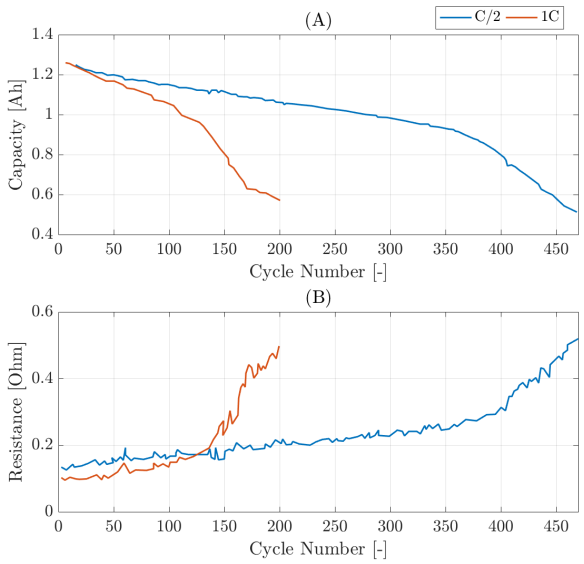

Fig. 5: Effect of lithium plating on remaining capacity and internal resistance for two LCO cells: after a certain age lithium plating can start to occur, causing an increased degradation rate (inflexion point) in both capacity and resistance deterioration [51].

volume change induced mechanical stress, which can lead to anode structural damage (LAM), surface layer cracking (LLI and LAM), and contact loss with the composite electrode (CL). The active material's volume change may also result in a decrease in electrode porosity, which is required for the electrolyte to reach the bulk of the electrode. [21].

4) Transition Metal Dissolution

Most lithium batteries' cathodes contain transition metals such as iron, nickel, cobalt, manganese, and vanadium. Similarly, most battery electrolytes contain the salt $LiPF_6$. The cycling and storage of these cells, particularly at high cell voltages and high temperatures [55], can result in the formation of hydrogen fluoride (HF) from impurities inside the electrolyte, which increases the acidity of the electrolyte. The resulting HF corrodes the cathode and dissolves the transition metals, contributing to several degradational mechanisms in both the anode and the cathode, causing capacity fade and impedance rise. To begin, metal dissolution can cause structural degradation of the cathode (LAM), resulting in reduced lithium insertion capability [56]. Furthermore, after dissolution, the metals can migrate through the electrolyte and deposit on the anode, acting as catalyzers for the reductive decomposition reaction that causes SEI layer growth [57]. Finally, the deposition of transition metals on the anode during this reductive process may induce the formation of lithium metal dendrites on the deposited metals (LLI and LAM). These dendrites can cause internal short circuits, posing a significant safety risk.

Particularly spinel-containing chemistries, such as $LiMn_2O_4$ are vulnerable to transition metal dissolution, as the extent of dissolution can be much greater, resulting in more structural degradation of the cathode (LAM). Although transition metal dissolution is unavoidable during the charging process, it can be reduced by reducing impurities in the electrolyte, using dopants, and using protective coatings around the cathode to reduce direct contact between the cathode and the electrolyte. [57].

5) Other Ageing Mechanisms

Other degradation mechanisms at the anode include graphite exfoliation: the structural degradation of graphite (LAM) as a result of high current densities or solvent co-intercalation, particle cracking (LAM) as a result from mechanical stress or high current load, binder decomposition (CL) caused by high temperatures and high cell voltages, corrosion of current collectors (CL) and loss of electrical contact (CL). For more details, interested readers are direct to [21], [32], [51].

6) Lithium-Titanate-Oxide and Silicon-based Anodes

The main advantage of Lithium-Titanate-Oxide (LTO) anodes over graphite anodes is their higher potential, as shown in Figure 4. As a result, these anodes are not thermodynamically unstable and therefore do not form an SEI layer [58]. Furthermore, LTO is a zero-strain material that does not change volume when charged or discharged. As a result, LTO-anode batteries can handle extremely high C-rates while still retaining a long lifetime. This comes at the cost of a lower energy density due to their higher potential [59].

On the other hand, silicon (Si) based anodes have a superior energy density, with a theoretical capacity of 3580 mAh/g, compared to 350mAh/g for graphite-based anodes and 175mAh/g for LTO-based anodes [60]. However, during cycling, the volume of the silicon particles can change by up to 280 percent. These volume changes cause excessive mechanical stress, reducing their lifetime significantly [34].

B. Cathode Ageing

The cathode is the lithium-containing part of a cell, and the limiting factor during charging as its maximum voltage determines the end of charge voltage. Similarly, the anode is the limiting factor during discharge due to its minimum discharge voltage limit [32], [61]. In terms of ageing, the cathode is generally regarded as less significant [62], [63].

Common cathode chemistries are LCO, LFP, NMC, LMO and NCA. These chemistries all have their strengths and weaknesses, varying in energy- and power-density, toxicity, safety, cost and natural abundance, among other things. Although many more chemistries exist, this review focuses on the most common materials.

The main ageing mechanisms of cathode materials include surface film formation, mechanical stress, and transition metal dissolution. Other ageing mechanisms on the inactive components include current collector corrosion, binder decomposition, and conducting agent oxidation [21], [54], as seen in Figure 3. The most significant ageing mechanisms are discussed below.

1) Cathode Surface Layer Film

Surface layer films (also known as Cathode Electrolyte Interphase (CEI) layer) can form on the cathode, similar to the anode, but due to electrolyte oxidation and salt deposition [21], [64], [65]. In contrast to the SEI layer, the cathode surface layer shows low lithium-ion conductivity, increasing the impedance. Furthermore, also gas evolution is possible

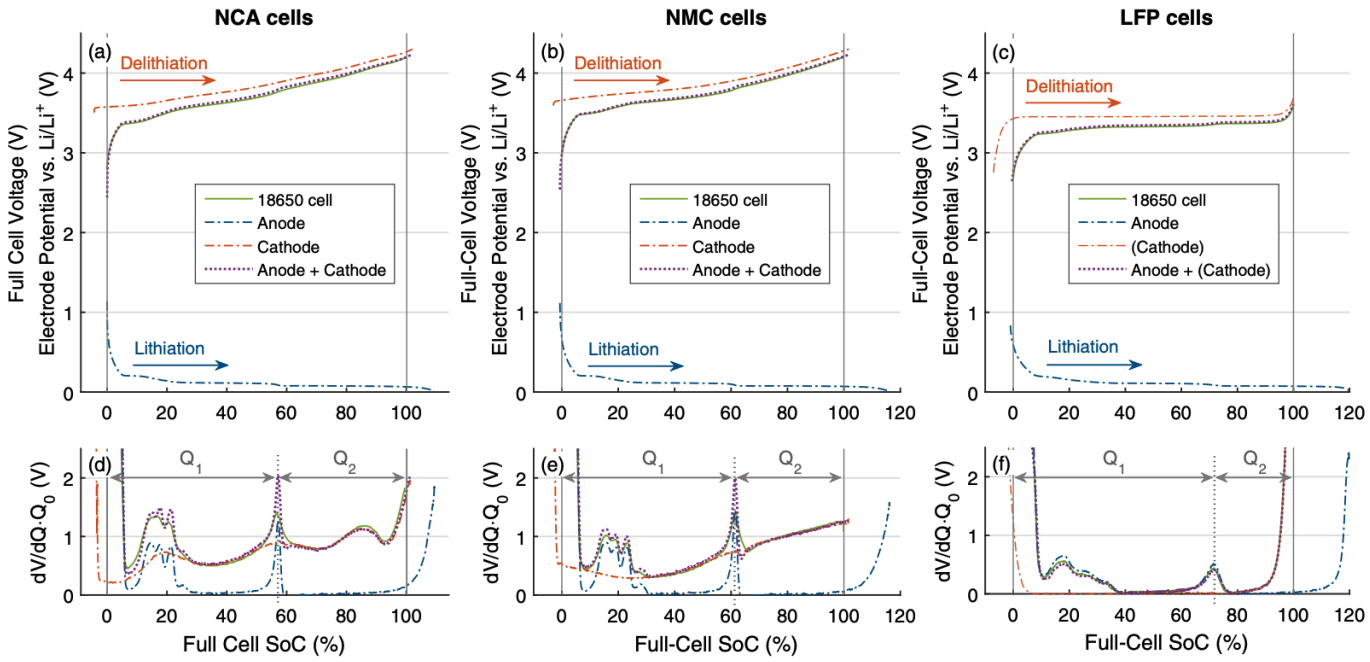

Fig. 6: (a-c): Voltage and differential voltage profile of an NCA (a), NMC (b), and LFP (c) full cells during low current charging, including a reconstructing of full cell voltage based on half-cell voltage profiles (dotted lines). (d-f): Differential voltage spectra of the three different cells. Figures (c) and (f) show that the cathode voltage profile of an LFP cell is very flat compared the other two chemistries, due to the two-phase regime. The figure is obtained from the publicly available material of P. Keil et al. in [23], under the Creative Commons Attribution 4.0 License CC-BY.

[21], [51]. According to the authors of [51], organic products formed by reduction at the anode may also be transported to the cathode, where they are oxidized and deposit on the cathode surface, resulting in LAM and LLI. Similar findings have been made in [66]. Unfortunately, due to the higher voltage of the cathode, this surface film layer is more difficult to detect [64], [65].

2) Mechanical Stress at Cathode

The cathode, like the anode, can go through phase transitions during the intercalation and deintercalation of Li-ions, which can result in LAM and CL. The amount of volume change varies depending on the chemistry. LFP cells, for example, only have a two-phase regime consisting of $FePO_4$ and $LiFePO_4$ [67]. As a result the (cathode) voltage and differential voltage profile of these cells is very flat, as shown in Figure 6. Because of this two-phase regime, LFP cells exhibit only a slight increase in volume, around 6.8% [1] and have a very high rate capability as well as a good lifetime [67]. Other chemistries, such as NCA or NMC, show multiple phase transitions in both cathode and anode voltage profiles. Manganese-containing chemistries, particularly LMO, exhibit additional mechanical stress as a result from Jahn-Teller distortion of Mn3+ particles. This results in a phase change from cubic to a tetragonal form. In the case of LMO, this can increase the cathode volume by approximately 16% [2], [21] resulting in additional LAM [68], [69]. Jahn-Teller Distortion occurs at low SoC. By controlling the end-of-discharge-voltage (EODV) and adding dopants, the capacity fade caused by volume change can be reduced .

3) Transition Metal Dissolution

As mentioned above, transitions metals in the cathode can dissolve resulting in structural degradation of the cathode (LAM).

III. Review of Empirical Degradation Modelling

This section discusses the most common empirical and semi-empirical modelling techniques and their limitations. Furthermore, the cells' ageing behaviour is discussed, and where possible, explained using the described degradation mechanisms. LIB degradation can be divided into two different types:

- Calendar ageing: the ageing which occurs when the cell is in an idle state. Calendar ageing results from side reactions that take place due to thermodynamic instability of the materials [51].
- Cyclic ageing: includes the ageing as a result of cycling the battery. Various kinetically induced effects, such as volume variations or concentration gradients, result in additional degradation [39], [51].

Following the reviewed studies, this paper focuses more on capacity fading than resistance increase. A summary of all studies and their testing conditions can be found in Tables II,III, and **??**.

A. Calendar Ageing

Capacity fading due to calendar ageing can be separated into two parts: reversible and irreversible capacity loss. By recharging the battery, the reversible part can be restored,

This article has been accepted for publication in a future issue of this journal, but has not been fully edited. Content may change prior to final publication. Citation information: DOI 10.1109/TTE.2021.3138357, IEEE Transactions on Transportation Electrification

whereas the irreversible part cannot. This review focuses on the irreversible part of calendar ageing. Reversible capacity loss is studied in more detail in [70], [71]. The three factors that influence calendar ageing are 1. Temperature, 2. SoC and 3. Time. In the following sections, the impact of these stress factors will be discussed separately. However, it is important to note that their degradation behaviour is not entirely independent of one another but is strongly correlated. A summary of all reviewed calendar ageing models, including their range of test conditions is shown in Table II.

1) Time

III-A1a Modelling Techniques: Time

It is widely reported in the literature that the major degradation effect for graphite anode based LIBs is the formation and growth of the SEI layer [66], [73], [84], [85], [90], [91]. As mentioned above, SEI layer growth is generally associated with a $\sqrt{\text{time}}$ ageing behaviour. To this extend, the time dependency off calendar ageing is most often modelled using a power-law relationship with z in a range of 0.5 to 0.8 [73], as shown in Eq.(1).

$$Q_{loss} = f(SoC, T)t^z \tag{1}$$

Where,

- Q_{loss}: lost charge.
- $f(SoC, T)$: function describing the state of charge and temperature dependency of calendar ageing
- t: time
- z: power exponent

An example of a corresponding degradation curve is shown in Figure 7. The exponential or pre-exponential components are often functions of SoC and temperature. In general, a higher SoC or higher temperature results in an increased calendar degradation rate. At a higher SoC, more lithium is intercalated in the anode resulting in a lower anode potential (V vs. Li/Li+) [2] and higher reaction rate. Similarly, as the particle collision rate increases at higher temperatures, the reaction rate increases. This is confirmed by the results of [13] shown in Figure 7. It also shows that for a lower SoC the capacity retention follows a more linear curve. Comparable results were observed in [72]–[74], [83], [92]. A possible explanation for the linear decay is cathode surface film growth, which has a non-passivation character. Therefore its reaction rate does not decrease over time [3] [93]. Another explanation could be transition metal dissolution as a result of high-temperature storage.

III-A1b Modelling Limitations & Challenges: Time

An occasionally observed result is a slight increase in capacity when the cell is still relatively new. This is most commonly observed for lower SoC storage, but is also observed under cycling conditions [13], [70], [83], [84], [94]. Again this is also shown in Figure 7, for the 0% and 10% SoC lines. After this initial increase in capacity, the capacity fading generally follows a similar trend as for other conditions, and therefore the found empirical fit is often still valid, even though it has been offset by the initial increase. The authors of [84] mention electrochemical milling as a potential cause for the increase in capacity. In [95] the so-called relaxation effect, due to the long resting period after cycling, is mentioned as a possible explanation. This relaxation effect can be caused by a change in local charge equilibrium, a drop in concentration gradient of active material and electrolyte, and a change in double-layer capacitance structure. Another explanation given in [70] denotes the passive electrode effect as a possible explanation; here, a slow movement of active lithium particles between the passive and active part of the anode is given as an explanation for the rise in capacity.

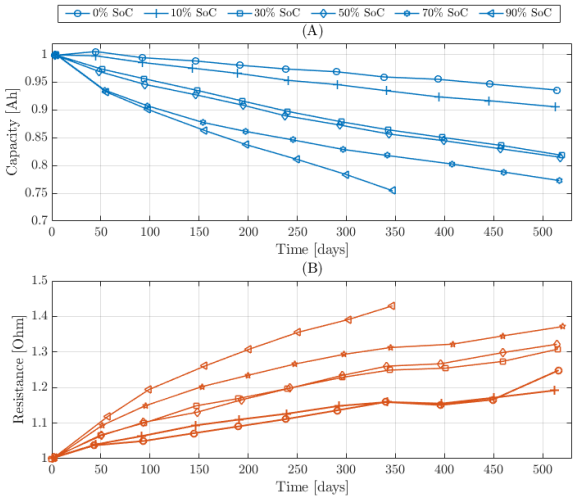

Fig. 7: Normalized capacity and resistance over time for calendar ageing test of NMC cells performed at 50°C and various SoC [13]. Their results show a clear correlation with SoC, where higher storage level results in higher degradation rate.

III-A1c Key Insights On the Effect of Time

The effects of time on the calendar ageing of LIBs can be summarized as follows:

- SEI layer growth is reported as the main cause for the degradation rate following a $\sqrt{time}$ curve. Higher temperature and SoC result in a faster degradation rate.
- At lower SoC, the degradation of the cathode might be an explanation for the more linear decay of capacity.
- An initial increase in capacity is occasionally observed. Different explanations for this phenomenon are given in literature.

2) Temperature (Calendar)

The most critical stress factor for LIB degradation is temperature; all reaction rates, parasitic and non-parasitic, are related to temperature. It, therefore, affects all other stress factors.

III-A2a Modelling Techniques: Temperature (Calendar)

The most common semi-empirical technique to model the degradation due to temperature is using the Arrhenius law [74],

[2]lithium metal composites have a negative potential; therefore, voltages are measured with respect to this potential

[3]A material becoming passive means that it is getting less affected or corroded by its environment

TABLE II: Overview of studies investigating empirical and semi-empirical calendar life models @

Study	Chemistry	Capacity	Resistance	Factors	Conditions		
					Temp.	SoC	Time
[72]	LFP	✓	x	SoC, T, time	30-60°C	30-100%	850 days
[73]	LFP	✓	x	SoC, T, time	40-55°C	10-90%	800 days
[74]	LFP	✓	✓	SoC, T, time	30-60°C	30-100%	450 days
[75]	LFP	✓	x	SoC, T, time	30-50°C	30-90%	300 days
[63]	LFP	✓	✓	SoC, T, time	30-60°C	30-100%	225 days
[76]	LFP	✓	✓	SoC, T, time	25-55°C	30-100%	305 days
[77]	LFP	x	✓	SoC, T, time	40-55°C	10-90%	225 days
[78]	LFP	✓	x	SoC, T, time	40-60°C	40-80%	105 days
[79]	LFP	✓	x	SoC, T, time	40-55°C	10-90%	-
[80]	NMC	✓	✓	SoC, T, time	30-60°C	30-100%	480 days
[81]	NMC-LMO	✓	x	SoC, T, time	60°C	10-100%	252 days
[82]	NMC-LMO	✓	✓	SoC, T, time	30-50°C	30-90%	290 days
[83]	NMC	✓	✓	SoC, T, time	0-45°C	25-100%	450 days
[13]	NMC	✓	✓	SoC, T, time	35-50°C	0-100%	520 days
[84]	NMC	✓	x	SoC, T, time	35-50°C	0-100%	520 days
[85]	NMC	✓	✓	T, time	10-46°C	50%	520 days
[86]	NMC-LMO	✓	✓	T, time	30-60°C	30-100%	1200 days
[87]	NCA	x	✓	SoC, T, time	30-55°C	90-110%	219 days
[88]	-	✓	x	SoC, T, time	30-60°C	30-100%	800 days
[89]	-	✓	x	SoC, T, time	0-60°C	5-100%	9 year

[83], [92], [96], given in Eq.(2). The Arrhenius law models the effect of temperature on chemical reaction rate.

$$k = A \exp \frac{-E_a}{RT} \tag{2}$$

Where,
- k is the reaction rate constant
- T is the absolute temperature
- A is the pre-exponential factor
- E_a is the activation energy
- R is the universal gas constant

The activation energy here refers to the additional energy required for a reaction to take place. The Arrhenius equation is often related to the rate of all parasitic side reactions leading to SEI growth [21] in LIB ageing research. Other models based on exponential or power-law relationships are also often utilized [36], [86].

III-A2b Modelling Limitations & Challenges: Temperature (Calendar)

Based on the summary of the testing conditions presented in Table II it is clear that the majority of the papers have investigated accelerated calendar ageing at elevated temperatures, ranging from 30°C-60°C. This is probably done to reduce the calendar life to a better manageable period. However, this raises the question of whether the ageing rate at 50°C-60°C is translatable to the ageing rate at 15°C-25°C. A rule of thumb is that the ageing rate doubles for every 10°C Celsius increase in temperature [13], [73], [86], [92], [96]. For studies using the Arrhenius law, this would result in an activation energy close to 50 kJ/mol. In some cases, this assumption is even used to derive the ageing model [97]. To test this hypothesis, the ageing data of the reviewed studies is sampled and analyzed according to Eq.(3).

$$\alpha = \frac{C(T_2)}{C(T_1)} \frac{10}{T2 - T1} \tag{3}$$

Here,
- $\frac{C(T_2)}{C(T_1)}$: the ratio of percentage capacity loss between temperatures.
- $T_{1,2}$: temperatures of samples 1 and 2.
- α: factor to test the hypothesis.

An α equal to 2 would indicate twice as much capacity degradation for every 10°C Celsius. Using Eq.(3) the data of each study is compared, only to cells from the same study, tested at the same SoC, and measured around the same time, such that only the temperature is variable. Figure 8 concludes

that the given hypothesis often overestimates the calendar ageing, as the peak occurs at approximately $\alpha = 1.5$, which means that most tested cells increase ageing by 50% every 10°C. Further investigation did not show any other correlation between age or SoC.

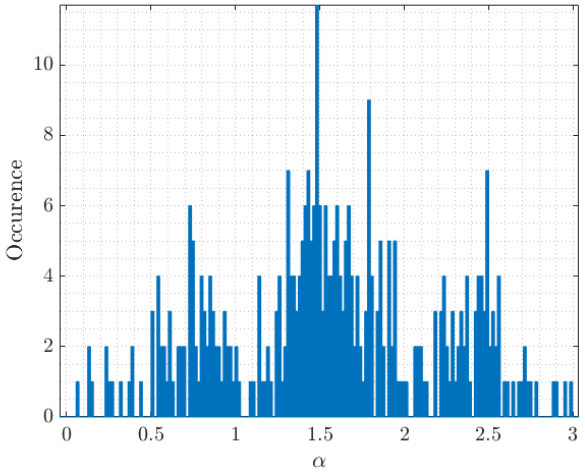

Fig. 8: Found results for α of Eq.(3). In the tested studies, 60% of calculated values of α were below 2, and a peak around $alpha = 1.5$ was observed, which means that most tested cells have an increased ageing rate of 50% for every 10° increase. The spread of values confirms the interdependency with other stress factors such as age and SoC, however, no clear correlation was found

Due to the complex nature of LIB degradation, it is challenging to give a rule of thumb figure as the ageing rate will always depend on multiple correlated factors. For this reason, the testing conditions, especially temperature, should be as close as possible to the operating conditions of the application, as extremely high temperatures result in different ageing mechanisms and therefore different ageing behaviour. An example of this is shown in [86]. Here the authors show that for an NMC cell stored at a temperature of 60°C, the ageing rate increases tenfold when the cells are stored at 100% SoC compared to 20% SoC. In comparison, this difference at 30°C Celsius is negligible. A possible explanation could be the restructuring of the SEI layer as it starts to break down at higher temperatures, dissolves and re-precipitates. Furthermore, in [21] it is also reported that organic SEI products are changed into more stable inorganic products, thereby reducing the reaction rate but also reducing the ionic conductivity of the SEI and thus increasing the resistance.

III-A2c Key Insights On the Effect of Temperature (Calendar Ageing)

The effects of temperature on the calendar ageing of LIBs can be summarized as follows:

- The Arrhenius law (or similar exponential forms) is the most common form of modelling the temperature dependency of calendar ageing.
- Temperature has a strong influence on all other stress factors and ageing mechanisms. To this extend, test conditions should be as close as possible to operating conditions in order to avoid modelling errors.

3) State-of-Charge (Calendar)

The last stress factor related to calendar ageing is the SoC (or analogously terminal voltage). Table II shows strong similarities between studies regarding testing conditions since most studies have modelled the effect of SoC based on three to four conditions.

III-A3a Modelling Techniques: SoC (Calendar)

In [80], the authors have modelled the SoC dependency as a polynomial function, where the interdependency of temperature and SoC is included by multiplication, as shown in Eqs.(4)-(6).

$$G(t) = A(T, SoC)e^{B(T,SoC)t} + Ce^{Dt} \tag{4}$$

with,

$$A(T, SoC) = a_1 \cdot SoC + a_2 \cdot T + a_3 \cdot SoC \cdot T \tag{5}$$

$$B(T, SoC) = b_1 \cdot SoC + b_2 \cdot T + b_3 \cdot SoC \cdot T \tag{6}$$

Here,

- $G(t)$: calendar ageing over time
- SoC: state of charge
- T: temperature
- $A(T, SoC), B(T, SoC)$: function to model temperature and SoC interdependency
- a_{1-3}, b_{1-3}, C, D: curve fit parameters

In [36], [98] calendar ageing is modelled as exponentially dependent on SoC, following Eq.(7).

$$A_{cal} = A_0 e_0^{\frac{SoC - SoC_0}{b}} e^{\frac{T - T_0}{c}} \sqrt{t} \tag{7}$$

Here,

- A_{cal}: calendar lifetime
- A_0: specified calendar lifetime under conditions SOC_0 and T_0
- b, c: curve fit parameters

Eq.(8) shows how [72], [99]–[101] modelled the pre-exponential factor in the Arrhenius law to be SOC dependent. [72], [99] also model the activation energy to be dependent on SoC, as shown in Eq.(8).

$$Q_{loss}(t, T, SoC) = Ae^{B \cdot SoC} \cdot e^{\frac{-E_a + C \cdot SOC}{kT}} t^z \tag{8}$$

here,

- Q_{loss} : lost charge
- A,B,C : curve fit parameters
- k: Gas constant
- T: temperature

In [74] the authors observed a linear increase for the SoC-dependent degradation. Therefore the kinetic dependency of (T, SoC) is modelled using an Arrhenius equation multiplied by SoC. The SoC dependency of calendar age-induced capacity degradation is modelled as a power-law relationship in [73], [79], [89], [96]. In contrast, the decrease in power capability is modelled in a linear relationship in [79].

Although diverse modelling methodologies are documented in the literature, the general trend suggests an increase in degradation with increasing SoC, especially at higher temperatures, [13], [86].

III-A3b Modelling Limitations & Challenges: SoC (Calendar)

Most reviewed studies only perform tests with three to four different SoC conditions due to practical constraints on testing capacity. This incorrectly leads to the belief that the rate of capacity and resistance deterioration for higher SoC's increases continuously. However, in [39], [96] calendar ageing was investigated with a higher resolution in SoC. Both these studies found a direct correlation between the graphite anode potential and capacity ageing.

In Figure 9 the results of [39] are shown for three different chemistries. As expected, an increase in storage temperature increases the capacity fading. However, more importantly, the results also show different plateaus with respect to storage SoC. There seems to be a direct correlation between the rate of capacity fading and the graphite anode stages for all three chemistries. These stages occur due to the different compositions of the lithium and carbon molecules, resulting in a different volume and potential. A schematic representation of the different stages, along with the anode potential during charge and discharge, is shown in Figure 10 [102].

The results of [39], [93] confirm that SEI growth results from electrochemical instability of the electrolyte-electrode interface. In both studies, these plateaus were not observed in the resistance increase. For the LFP cell this increased independently of SoC, whereas the rate of resistance increase for the NMC and NCA cells was found to be substantially larger at higher SoC, especially around 90-100%. The cathode surface film layer could be a possible explanation, which for LFP cells is much less SoC dependent due to the more stable crystal lattice and two-phase regime. Based on the results of [39], [96] it can be concluded that curve fitting the SoC dependency with only three test conditions is insufficient to accurately capture capacity fade as a function of SoC, as it will lead to significant under- and overestimations in certain SOC regions. The advantage, however, is that the anode potential can be determined prior to performing the ageing test. For example, the anode potential or differential voltage analysis (DVA) can be used. Once the anode potential is known, the choice of SoC testing conditions can be made strategically. Furthermore, knowing where the phase transition occurs during the operation of a LIB can help reduce calendar ageing.

Another observation on the results shown in Figure 9 is the drastically increased ageing at 100% SoC for the NMC chemistry. This was not observed in the other chemistries, and similar results have been found in other ageing studies of NMC cells [84], [86], [92], [96]. The increased ageing appears to be independent of anode potential. A possible explanation could be other degradation mechanisms driven by a high cell voltage, such as electrolyte oxidation, transition-metal dissolution, or structural damage to the cathode due to a high degree of lithiation [103], [104]. Due to the disproportionate increase in ageing at high temperature and very high SoC ($\geq$95%) it is not recommended to test NMC cells at 100% SoC, if the amount of testing conditions is limited as it will result in large overestimations for conditions below 95% SoC.

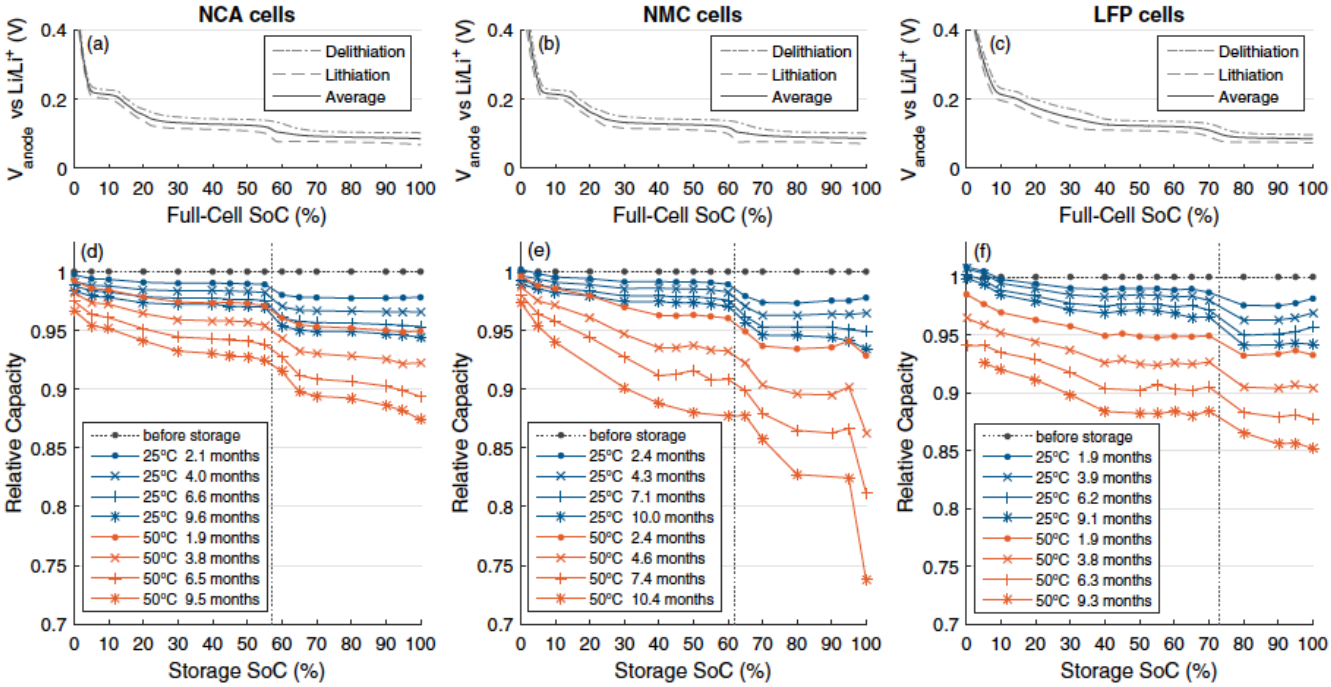

Fig. 9: Graphite anode potential vs. SoC of three different half-cells [4]. A strong correlation between anode potential and degradation rate is observed for all cells, especially the phase transformation around 60-70% marks a significant change in degradation rate.. The figure is obtained from the publicly available material of P. Keil et al. in [39], under the Creative Commons Attribution 4.0 License CC-BY.

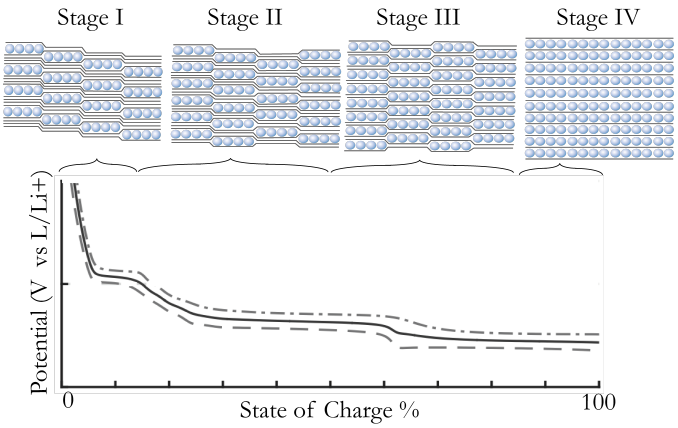

Fig. 10: Schematic representation of the staging phenomena observed at the anode [102]. Because the arrangement of carbon and lithium molecules differs in each phase, each stage has a different potential and volume, and therefore a different degradation rate.

III-A3c Key Insights On the Effect of SoC (Calendar Ageing)

The effects of SoC on the calendar ageing of LIBs can be summarized as follows:

- The anode potential appears to be the main factor determining the rate of degradation in graphite-anode-based cells. This demonstrates that SEI layer growth is the dominant ageing mechanism for these cells.
- Modelers should be cautious when developing models based on a limited number of testing conditions. Because the degradation rate is determined by the anode potential, which is not a continuously changing potential but instead follows the stages determined by the anodes' phase transitions.
- A significant amount of studies testing NMC cells at 100% SoC, observed a disproportionate increase in ageing, for a slightly lower SoC. To this extent, higher accuracy over the entire SoC range can be achieved when the maximum SoC tested is 90-95%.

B. Cyclic Ageing

Table III summarizes the cycling ageing studies and their testing conditions. The relevant part is discussed in the accompanying section for studies that discuss both calendar and cyclic ageing.

1) Combining Cyclic and Calendar Ageing

Based on the reviewed studies, no single idea about the correlation between calendar and cyclic ageing can be derived. In [86], ageing is modelled using Dakin's approach. Here cyclic and calendar ageing are modelled to be multiplicative. The authors of [13], [21], [78], [98] have mentioned that cycling results in additional (cyclic) degradation due to added mechanical stress and lithium plating. Furthermore, various studies show that the SEI layer's growth and morphology alter according to the operating conditions. During cycling conditions, the SEI layer stays more porous, whereas a much denser layer is formed under storage conditions [46], [47], [96]. While cyclic and calendar ageing are mentioned to have a strong superposition for high temperatures or high SoC in [96], [105]. For milder conditions, especially at lower temperatures and increased C-rate, cycling ageing is probably dominant.

Note that studies that only discuss cyclic ageing have inherently incorporated calendar ageing as well. In this case, the superposition of calendar ageing is assumed to be non-existent [98], [106] or negligible compared to the cycling induced ageing. However, in these cases, the fast sequential cycling tests mask the effect of calendar ageing and, therefore, lead to estimation errors in applications with significantly more time between cycles. In practice, every modeller should determine the best practice for themselves, depending on their application and operating conditions.

2) Addressing Irregular Cycles: Rainflow Counting Method

Often, cyclic ageing studies are performed under fixed conditions. However, in reality, ageing is not as static as these test conditions. One way of dealing with highly irregular power profiles is using the rain flow counting method. Rainflow counting is a common fatigue analysis technique used to calculate the combined fatigue of a summation of different stress cycles. Several studies have used the rain flow counting method to calculate the combined degradation of an irregular power profile [42], [73], [94], [107], [108]. An example of this is shown in Figure 11. Here the rainflow matrix is shown for a randomly generated load profile, which shows the amount of cycles of a particular current rate [A] and throughput [A*s]. Other output quantities could be DoD, average SoC, or idle time. Next, the degradation can be determined based on the number of cycles with a specific amount of stress. The advantage of this technique is that it allows assessing the degradation of irregular profiles more accurately. However, it assumes that the sequence of cycles does not influence the outcome, e.g. the degradation due to a high DoD cycle followed by a low DoD cycle is similar to a low DoD cycle followed by a high DoD cycle. Furthermore, it assumes that the effect of a particular cycle (or sum of cycles) is independent of the current age of the battery. Interested readers are directed to [109] for more information on the rain flow counting technique.

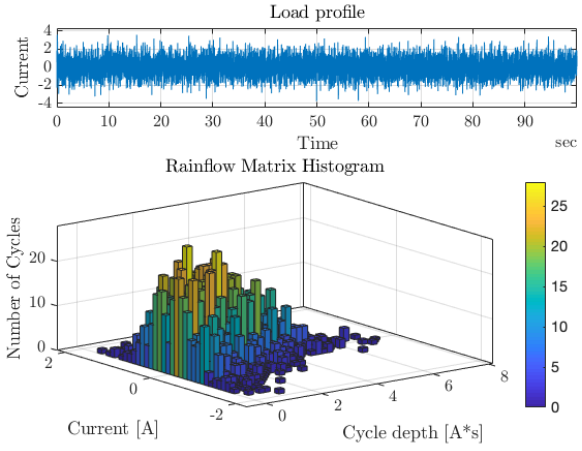

Fig. 11: Example of a rainflow matrix histogram based on a randomly generated load profile. In this case, the rainflow matrix counts the number of cycles of a specific cycle-depth with a specific current load.

TABLE III: Overview of studies investigating empirical and semi-empirical cycle life models

Study	Chemistry	Cap.	Res.	Factors	Conditions				
					Temp.	SoC	DoD	C-rate	Throughput
[94]	LFP	✓	x	SoC, DoD, C, Ah, T	25-40°C	30-70% (avg)	12.5-75%	1-1.82C	900 FEC
[73]	LFP	✓	✓	SoC, DoD, Ah, T	35-50°C	27.5-72.5% (avg)	10-60%	4C	1k-7k FEC
[110]	LFP	✓	x	DoD, C, T	-30-60°C	100% (start)	10-90%	0.5-10C	1k-6.5k FEC
[111]	LFP	✓	✓	DoD, T, C	-18-40°C	100% (start)	20-100%	1-15C	550-2900 FEC
[41]	LFP	✓	x	T, Ah, C	25°C	100% (start)	100%	0.5-5C	550 FEC
[97]	LFP	✓	x	T, Ah, C	25°C	100% (start)	100%	0.5-5C	1.2k-10k
[112]	LFP	✓	x	SoC, T, Ah, C	36-45°C	38.5-60% (avg)	100%	2.82-6C	4k-20k FEC
[113]	LFP	✓	✓	SoC, DoD, T, Ah	30, 45°C	1.25V-2V 3.65V-3.95V	100%	4C	200 FEC
[105]	LFP	✓	✓	DoD, Ah, C	30°C	100% (start)	5-100%	1-3.5C	2k-5.5k FEC
[114]	LFP	✓	x	SoC, Ah, C	55°C	0-30%	10-30%	4-8C	3.9k-12.5k
[115]	LFP	✓	x	C, T	25,45°C	100% (start)	100%	1C	4.5k FEC
[79]	LFP	✓	✓	SoC,DoD, T	35-50°C	10-90% (start)	10-80%	4C	8k
[78]	LFP	✓	✓	C, Ah,	25°C	40-80% (start)	3,6%	0.5-1C	-
[116]	LFP	✓	x	SoC,T, C,Ah	22.8°C - 51.6°C	100% (start)	60,100%	1-4C	654-4286 FEC
[117]	LFP	✓	✓	x	22.8°C - 51.6°C	100% (start)	60,100%	1-4C	654-4286 FEC
[101]	LFP	✓	x	T, C, Ah	40-50°C	60-85% (start)	20-65%	0.4-4C	4k
[42]	LFP	✓	x	SoC,DoD,T, Ah	20°C	75-100% (start)	50-75%	1C	4k-8k FEC
[118]	LFP	✓	✓	SoC, Ah,	5, 44°C	100% (start)	100%	1.5C	990 FEC
[42]	NMC	✓	x	SoC,DoD,T, Ah	20°C	75-100% (start)	50-75%	1C	4k-8k FEC
[118]	NMC	✓	✓	SoC, Ah,	5, 44°C	100% (start)	100%	1.5C	990 FEC
[13]	NMC	✓	✓	SoC, DoD, Ah, T	35°C	10-95% (avg.)	5-100%	1C	1.5-4.5k FEC
[86]	NMC	✓	✓	DoD, Ah, T, C	40,50°C	100% (start)	20-40%	10,20C	-
[84]	NMC	✓	x	SoC, DoD, C, T	-10-50°C	20-80% (avg.)	10-100%	1/3-2C	900-1k FEC
[119]	NMC	✓	x	SoC, T, Ah, C	10-45°C	100% (start)	55-75%	1/3-5C	800-1400 FEC
[93]	NMC	✓	✓	SoC, T, Ah, C	10-45°C	40-70% (avg)	20%	5-20C	-
[120]	NMC	✓	x	SoC, T, Ah, C	10-46°C	100% (start)	50%	0.5-6.5C	1.3k-1.7k FEC
[85]	NMC	✓	x	T, Ah, C	10-46°C	100% (start)	10-90%	0.5-6.5C	900-4.3k FEC
[92]	NMC	✓	✓	SoC, DoD, T, Ah, C	40°C	5-90% (avg)	10,60%	1C	2k FEC
[82]	NMC/LMO	✓	✓	SoC, T	30-50°C	100% (start)	10-70%	4C	-
[101]	NCA	✓	x	T, C, Ah	40-50°C	60-85% (start)	20-65%	18C	4k
[86]	NCA	✓	✓	DoD, Ah, T, C	40,50°C	100% (start)	20-40%	9,16C	-
[121]	NCA	✓	✓	SoC, DoD, Ah, T	20°C	EOCV: 3.9V-4.1V	20-80%	9,16C	-
[122]	NCA	✓	x	SoC, DoD, T	20°C	80,100% (start)	60-80%	-	782 FEC
[123]	NCA	✓	x	DoD, T, Ah, C	0-50°C	EEODV: 2.4-2.5V EOCV: 4.1-4.3V	60-80%	0.2-1C	782 FEC
[42]	LMO	✓	x	SoC,DoD,T, Ah	20°C	75-100% (start)	50-75%	1C	4k-8k FEC
[118]	LMO	✓	✓	SoC, Ah,	5, 44°C	100% (start)	100%	1.5C	990 FEC
[100]	LMO	✓	x	SoC, T,	25°C	35-50% (avg.)	20-95%	1C	900 FEC
[124]	LMO	✓	x	Ah	25°C	100% (start)	100%	1C	700 FEC

Study	Chemistry	Cap.	Res.	Factors	Conditions				
					Temp.	SoC	DoD	C-rate	Throughput
[125]	LMO	✓	x	DoD, T, C	20-50°C	100% (start)	20-100%	1-5C	900 FEC
[126]	LCO	✓	x	SoC, DoD, T, C	25°C	EOCV: 4.1V-4.3V	100%	0.5-1.4C	900 FEC
[127]	LCO	✓	x	DoD, T, Ah, C	25-45°C	100% (start)	20-30%	0.6-1.2C	500-800 FEC
[89]	LCO	✓	x	SoC, DoD, T	0-60°C	0-100% (start)	3-80%	1/5C	10k FEC
[128]	LCO	✓	x	Ah, C	-	100% (start)	100%	0.5-1C	550 FEC
[129]	LCO	✓	x	SoC, C	25°C	EOCV: 4.2-4.35	100%	1C	250-500 FEC

3) Throughput

Throughput describes the net Ah delivered by the battery over multiple cycles. As a result, it is one of the critical stress factors for cycling ageing.

III-B3a Modelling Techniques: Throughput

Similar to time for calendar ageing, the relationship for throughput is often modelled using a power-law relationship [13], [41], [101], [110], [112], as described in Eq.(9) or Eq.(10). Furthermore, throughput is also modelled in terms of number of cycles combined with depth-of-discharge. Often with similar power-law equations [73], [84].

$$Q_{cycl} = f(SoC, T, DoD, I)Ah^z \tag{9}$$

$$Q_{cycl} = f(SoC, T, DoD, I)N_{cycle}^z \tag{10}$$

Where,

- $f(SoC, T, DoD, I)$: degradation due other stress factors.
- Ah: the total cumulative throughput of the cell.
- N_{cycle}: the amount of performed cycles, sometimes expressed in terms of depth-of-discharge.
- z: power-law exponent.

The typical values of z are in the range of 0.5-0.8, which is generally associated with SEI layer growth. The authors of [13], found the best fit for z around 0.5, after subtracting calendar ageing. Meaning that as the battery ages, the SEI thickens, and the capacity fade due to cycling induced stress on the SEI decreases. In [127] values of z in the range of 0.8 have been reported, following a less logarithmic and more linear degradation rate. A possible explanation could be an increased share of cathode surface layer film growth [93]. In [114], the authors found the best curve fit using $z = 1.23$. Here the degradation due to the charge-sustaining (CS) mode of plug-in hybrid electric vehicles (PHEV) has been investigated. Here the CS mode of a PHEV was characterized by low SoC and very high C-rates. The resulting degradation showed an increasing degradation rate, resulting in an exponential factor $z > 1$. Because of the low SoC, combined with the high C-rate, this increasing degradation rate is potentially dominated by metallic lithium plating, which in contrast to SEI growth, is a self-reinforcing process.

However, not all studies have reported non-linear cyclic ageing characteristics. In [94], [97] the cyclic degradation is modelled as linearly increasing with throughput, even though the results show a very slight saturation. Furthermore, in [122] cycling ageing is assumed to be linearly dependent on the number of cycles. This is, however, not confirmed by the experimental data shown in the paper. Finally, the authors of [46] have found a linear correlation between cycling induced capacity fade and the number of cycles (on top of a $t^{0.5}$ time dependency). A destructive physical analysis showed that damage to the cathodes' active material was the leading cause for the cycle induced ageing. Additionally, the authors of [46] observed a linear increase in resistance, whereas the capacity fading showed a $t^{0.5}$ correlation. This indicates that the degradation mechanisms between capacity fade and resistance increase are different [13]. This difference between capacity and resistance deterioration was found in several studies [73], [96], [111], [119]. Unfortunately, no explicit explanation for this observation was given.

III-B3b Modelling Limitations & Challenges: Throughput

For studies investigating only cyclic ageing [73], [100], [110], [112], [119], it could be argued that the superposition of calendar ageing has a strong effect on their results, especially at higher temperatures and SoC. According to [110], [127], time is inherently incorporated in throughput, as every charging instance with a particular C-rate is also a function of time. However, this is only valid if the cell is cycled continuously, which is rarely the case in practical applications.

Most of the above-described studies use some form of the Arrhenius equation, combined with a power-law relationship on throughput or number of cycles. This form of modelling is generally well suited to predict ageing due to long term storage or cycling during a post-process calculation. However, for online calculations over a shorter period, or fast-changing operating conditions, it is less suited as the current age of the battery is not taken into account at every new iteration/calculation. This has been resolved by the authors of [101] by differentiating the Arrhenius/Power-Law over time. Starting with Eq.(11), this results in the linearized form as shown in Eq.(12) [101].

$$Q_{loss} = B(I) \exp \frac{-E_a + \alpha|I|}{RT} Ah^z \tag{11}$$

$$\frac{Q_{loss}}{dt} = f(I, T) \left(\frac{Q_{loss}}{B(I) \exp \frac{-E_a + \alpha|I|}{RT}} \right)^{1 - \frac{1}{z}} \tag{12}$$

with,

$$f(I,T) = \frac{|I|}{3600} zB(I) \exp \frac{-E_a + \alpha|I|}{RT} \tag{13}$$

Another limitation of the Arrhenius/power law is that it only captures the degradation in the first stages of battery life, during which the degradation rate decreases as the battery ages. However, at a certain age, all LIBs experience an increase in degradation rate due to lithium plating, as shown in Figure 5. The authors of [84] model this inflexion point as a polynomial equation based on the number of cycles and DoD, according to Eq.(14). Figure 12 shows that this results in a good fit on their ageing data, and shows the inflexion points which start to occur around 3000 cycles. However, note that this is not observed in the data, and therefore the age at which plating starts to occur remains unknown.

$$RCD(x,y) = \sum_{i=0,j=0}^{n,m} a_i x^i + b_i y^i \tag{14}$$

Where:
- RCD: Relative capacity degradation (%)
- x: full equivalent cycle number
- y: DoD (%)
- a_i: constants for x
- b_j: constants for y
- n: order of x
- m: order of y

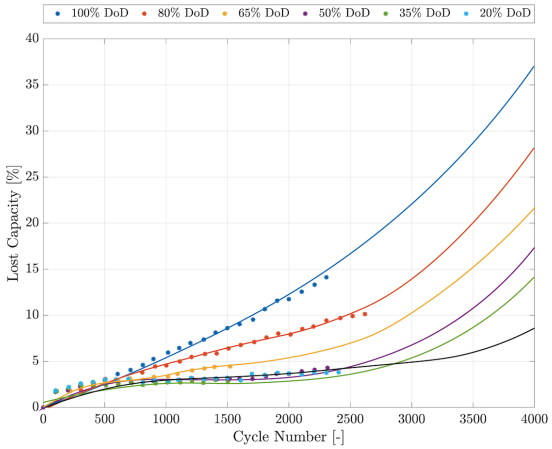

Fig. 12: Ageing and fitting result from [84]. In contrast to many exponential models this polynomial model takes into account the increasing degradation rate at later point in battery life, due to lithium plating.

Another option is to linearize the various stages seen in LIB life, such as done in [42]. Here the authors distinguish between four different stages, each modelled as linear functions dependent on various stress factors, see Figure 13.

III-B3c Key Insights on the Effect of Throughput

The most important insights on the effect of throughput can be summarized as follows:

- Often an Ah^z relationship, with $0.5 \leq z \leq 1$, is found for studies modelling the effect of throughput on cyclic ageing. Even though this may result in good accuracy in the first stages of battery life, it fails to capture the degradation in later stages, where an increased degradation rate is generally observed after an inflexion point.
- Studies investigating only cyclic ageing inherently include the effects of calendar ageing in their models. Depending on the application of the model, this can potentially lead to inaccurate results. Other studies have subtracted the expected amount of calendar ageing from their cyclic ageing test results to more accurately curve the ageing due to cycling.

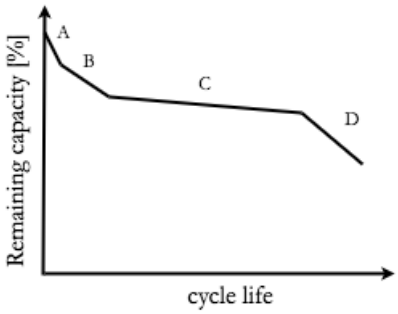

Fig. 13: Modelling battery degradation based on four different linear stages (stages (A)-(D)), this allows to linearize the degradation model over the entire lifetime of the battery [42]

.

4) Temperature

III-B4a Modelling Techniques: Temperature (Cyclic)

Also for cycling ageing the Arrhenius law [13], [41], [42], [84], [92], [110], or similar exponential relationships [73], [86], [97], are most often used to model the temperature dependent reaction rate. An example of an Arrhenius law model is given in Eq.(11). Also polynomial relationships, such as the example given in Eq.(15) and (16), are occasionally used [85].

$$Q_{loss} = B_1(T) e^{B_2(T) I_{rate}} Ah \tag{15}$$

with,

$$B_1(T) = aT^2 + bT + c, \quad \& \quad B_2(T) = dT + e \tag{16}$$

where:
- Q_{loss}: Lost capacity.
- T: Temperature.
- I_{rate}: C-rate.
- Ah: Throughput.
- a, b, c, d, e: curve fit parameters.

III-B4b Modelling Limitations & Challenges: Temperature (Cyclic)

In the studies mentioned above, good accuracies are achieved when using the Arrhenius law to model the temperature dependency at temperatures above room temperature. However, different to calendar ageing, the Arrhenius law is not a good indicator for the temperature-dependent degradation rate at

temperatures below room temperature [42], [86], [94] (and occasionally also at higher temperature rates [127]). Where for calendar ageing, lower temperatures reduce the reaction rate of parasitic side reactions, under cycling conditions, the lower temperatures also reduce the battery's ionic conductivity, leading to an increased impedance and reduced performance [130]–[132].

In [94], [133] a temperature around a $20-25°C$ was found to be the dividing limit at which the impedance starts increasing for lower temperatures, and above which the impedance decreases for lower temperatures. As a result, the least (cyclic) ageing is generally observed at around $20-25°C$ [84], [86], [94], [110], [111]. An example of this is shown in Figure 14, where the pre-exponential and exponential factors $B_1(T)$ and $B_2(T)$ from Eq.(15)((16)) are shown [85]. Therefore, cycling

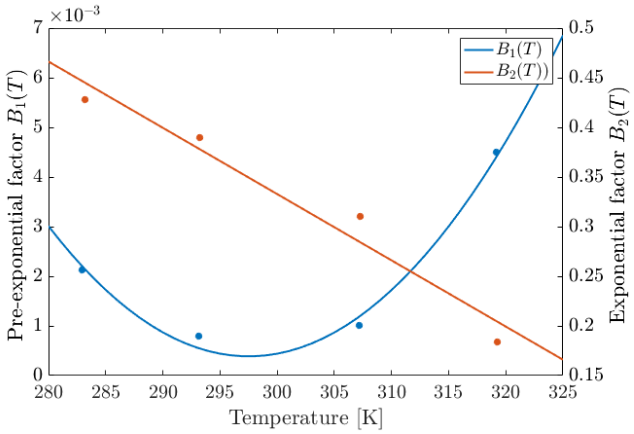

Fig. 14: The pre-exponential and exponential factors $B_1(T)$ and $B_2(T)$ from Eq.(15) show that the lowest degradation rate is observed for temperatures around room temperature. Additionally, a decreasing $B_2(T)$ shows that the effect of current rate decreases at higher temperatures. The shown results are obtained for NMC-LMO cells cycled at 50% DoD and 1C.

ageing models utilizing exponential relationships, fitted on test results above room temperature, can often not be used for conditions below a 20°C as this would result in severe underestimations. Nevertheless, the Arrhenius law can also be used at lower temperatures if combined with positive activation energy. An example obtained from [123], [134] is shown in Eq.(17).

$$Q_{loss} = A_L e^{\frac{E_a^L}{RT}} + A_H e^{\frac{-E_a^H}{RT}} \tag{17}$$

Here, the letters H and L denote the found parameters for high and low temperatures.

In [133] the authors showed, using post-mortem analysis, that different ageing mechanisms are dominant above and below 20°C for an NMC-LMO blended cathode cell. Their results show that lithium plating is the dominant ageing mechanism at low temperatures, caused by an increasing polarization near the electrode due to the slow diffusion and low ionic conductivity [47]. Whereas at higher temperatures, transition metal dissolution and SEI growth are the dominant ageing mechanisms. Similar results have been found in [135] for LCO cells.

A couple of studies have even performed ageing tests at subzero temperatures. However, most of them have not included these results in their models due to the extremely short cycle life (below 100 equivalent full cycles) [47], [84], [94], [110]. [131] Showed that the anode's diffusion rate is the main limiting factor at temperatures below zero. At temperatures above 20°C, the intercalation potential of graphite anodes often prevents lithium plating [135], until a certain age. At higher temperatures, active material loss and SEI growth are dominant [63], [136]. Especially, cathode chemistries containing manganese are sensitive to higher temperatures (and higher SoC) due to Mn-dissolution.

Not only the effect of temperature changes around $20-25°C$, also the interdependency of temperature with other stress factors such as C-rate. At higher temperatures, the impact of C-rates becomes less significant, as shown in Figure 14, and the effect of calendar ageing becomes more pronounced [86]. Whereas for lower temperatures, the detrimental effect of C-rate increases [85], [86]. More on this is discussed in the next section.

III-B4c Key Insights on the Effect of Temperature (Cyclic)

The most important insights on the effect of temperature can be summarized as follows:

- The majority of papers model the degradation rate to be exponentially dependent on temperature.
- Temperatures around $20-25°C$ are a tipping point below which a lower temperature increases the impedance and above which higher temperature increases the battery's impedance.
- As a result, models utilizing an exponential relationship to model the temperature dependency for cells cycled above room temperature might lead to significant underestimations when used for temperatures below room temperature. A possible solution could be to use both a positive and negative activation energy (or exponential factor).

5) C-rate

C-rate or the rate of (dis)charge is defined as the ratio of power (W) to energy capacity (Wh). Generally, higher C-rates are believed to be more detrimental to battery degradation. This has been confirmed in the majority of the reviewed studies, for C-rates above 2-3C. In [137] the authors cycled LCO cells with 1, 2, and 3C at room temperature. Using an electron microscope and impedance analysis, they showed that the increasing C-rates caused structural damage on the graphite anode of an LCO cell, resulting in the crack and repair of the SEI layer. The rate of capacity and resistance degradation was proportional to the C-rate. Similar results were found in [126], [127].

III-B5a Modelling Techniques: C-rate

In [85], [86], [111], [112], [120], among other studies, the authors modelled an exponential increase in degradation with respect to C-rate, often combined with an Arrhenius like equation, where the activation energy (or in general the exponential

component) is modelled as a linear function of C-rate as shown in Eq.(11) [101]. Others also included a linear dependency on C-rate in the pre-exponential factor [120], [127], as shown in Eq.(18).

$$Q_{loss} = A(C)e^{\frac{-E_a(C)}{RT}}n^{0.74} \tag{18}$$

with:

$$A(C) = e^{aC^2+bC+c} \tag{19}$$

$$E_a(C) = xe^{yC} + z \tag{20}$$

where:

- Q_{loss}: Lost capacity.
- T: Temperature.
- C: C-rate.
- Ah: Number of cycles.
- a, b, c, x, y, z: curve fit parameters.

The authors of [94], [97] inherently incorporated C-rate by using the normalized standard deviation in SoC ($SoC_{dev}(t)$) per time unit, as shown in Eq.(21)(22)

$$Q_{loss} =$$

$$k_1 SoC_{dev} \exp k_2 SoC_{avg} + k_3 \exp k_4 SoC_{dev} \tag{21}$$

Where,

$$SoC_{dev} =$$

$$\sqrt{\frac{3}{\Delta Ah_m}\int_A h_{m-1}^{Ah_m}(SoC(Ah) - SoC_{avg})^2 dAh} \tag{22}$$

Where,

- SoC_{dev}: the normalized deviation in SoC
- SoC_{avg}: the average SoC of a cycle.
- ΔAh_m: the amount of charge processed in cycle m.
- k_{1-4}: curve fit constants.

A different approach was taken in [112] (LFP), for C-rates of 2, 20 and 28C at temperatures above 36°C. The authors model the effect of C-rate to be more detrimental than temperature and SOC. Furthermore, according to their model, the impact of C-rate increases at higher temperatures. However, no accompanying data is shown to verify this. Note that the effect of cell self-heating becomes very significant at these C-rates, leading to increased calendar ageing due to significantly elevated cell temperature. Some authors even neglect the effect of C-rate, as it is incorporated in the temperature dependency [42]. This might be a valid assumption for lower C-rates, but for very high C-rates, the effect of mechanical and kinetic stress might be non-negligible.

III-B5b Modelling Limitations & Challenges: C-rate

Before discussing any limitations and challenges regarding C-rate dependent degradation, the authors would like to point out the differences between chemistries. LFP cells, for example, are well-known for their ability to handle large amounts of power. Furthermore, LIBs using LTO anodes can sustain extremely high C-rates with negligible degradation. However, when conducting cyclic ageing tests, readers and modellers should be aware of the effect of energy density on C-rate. As for the same cell size, with each equal electrode surface area, higher current densities are experienced for cells with a higher energy density for the same C-rate, potentially leading to an unfair comparison between cell chemistries [39].

Although most of the reviewed studies found an exponentially increasing degradation rate at C-rates above 2C, a significant part found a negligible increase in degradation for C-rates below 2C and temperatures between $30 - 45$°C, for both LFP and NMC chemistries [47], [84], [94], [105], [110], [119], [120], [125]. In [47] the increase in C-rate from 1C to 2C was found negligible at 45°, but non-negligible at 20°C. Showing the temperature dependency on C-rate. The authors report that the increased reaction rate and ion diffusion kinetics at these temperatures might reduce the stress caused by an increasing C-rate.

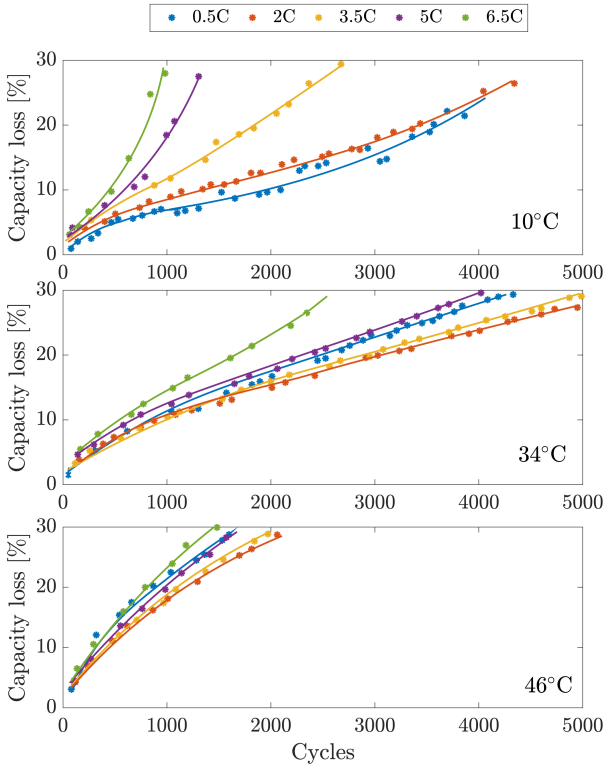

Fig. 15: Cycling ageing results of the NMC studies in [85]. The results show the interdependency of C-rate and temperature. At temperatures of 34°C and 46°C the effect of C-rate decreases and the least ageing is observed for 2C and 3.5C

To this extend, to adequately explain the effect of C-rate, a distinction between above and below room temperature should be made. At lower temperatures, the ionic conductivity and intercalation rate decreases [110], whereas the higher current density as a result of higher C-rate requires faster diffusion kinetics [47]. As a result, lower temperatures accelerate the detrimental effects of increasing C-rate, resulting in increased mechanical and kinetic stress on the electrodes and an increasing polarization gradient, potentially leading to lithium

plating [138]. Similarly, the effect of C-rate often decreases for increasing temperatures, as was found by the authors of [85]. Their results are shown in Figure 15. At 10°C it shows a clear dependency on C-rate, whereas for an ambient temperature of 34°C and 43°C the difference between C-rates decreased. Also, the capacity retention trajectory is distinctly different at 10°C and higher C-rates, pointing to an increasing rate of lithium plating. Finally, it is also noteworthy that the least ageing is not necessarily observed at the lowest C-rates.[5]. Nevertheless, also at higher temperatures, the effect of C-rate can cause detrimental effects such as crack propagation of the SEI layer, cathode overcharge (as a result of an increasing polarization gradient), or structural damage to the anode and cathode such as graphite exfoliation [32], [139]–[141].

Some authors have accounted for the interdependency between C-rate and temperature. In [86] NMC and NCA cells were cycled at temperatures of $40 - 50$°C and C-rates of 10 and 20C. The authors found an exponentially increasing degradation rate for higher C-rates. However, decreasing at higher temperatures. Therefore the temperature-dependent C-rate effect was modelled as a linear function of temperature, as shown in Eq.(23). Similar methods have been used in [85].

$$k_C = \exp\left(a(T)I\right) \tag{23}$$

Where,

- k_C: C-rate induced cyclic ageing.
- $a(T)$: Linear expression to describe temperature dependency of C-rate.
- I: C-rate.

III-B5c Key Insights on C-rate

From the above-described results, several conclusions can be drawn:

- The effect of C-rate is often modelled to be exponentially dependent.
- A strong interdependency with temperature is observed. Therefore, models obtained using temperatures above 20° are likely not to be valid at temperatures below this threshold due to an increasing impedance.
- For temperatures above 20°, the effect of C-rate decreases. Some studies even report less ageing is observed at higher temperatures or higher C-rates. Modelling C-rate a temperature-dependent function can therefore increase curacy.
- When performing cycling tests at very high C-rates, self-heating should be taken into account.
- Readers and modellers should be cautious when us exponential relationships with respect to C-rate, at C-r below 2. Several studies have shown that this relations is not valid for C-rates below the 2C threshold.

[5]More studies report less degradation at higher C-rates. In [105] (NMC), at 60% DoD the least degradation was observed for 3.5C, followed by 1C than 2C. Whereas at 100% DoD no difference was observed between 1C and 2C, and only a small difference was observed for cells tested with 10% DoD. All cycling tests were performed at 30°C. A complex correlation between C-rate and DoD was found; the authors mention that further investigation is required to determine this correlation

6) State of Charge (Cyclic)

Table III demonstrates that a considerable amount of studies did not investigate the effect of SoC on cyclic ageing, but instead always start their cycle at 100%. These studies are likely to have a larger calendar ageing superposition. Additionally, users should check whether this is suitable for their application, as battery management systems do not always charge the cells up to this point. The reviewed studies are divided into two categories: 1. Studies investigating the influence on End-of-Charge-Voltage and 2. Studies investigating the influence of average SoC.

III-B6a Modelling Techniques: End-of-Charge-Voltage

The final voltage at which the battery is maintained during the constant voltage (CV) charging region is the End-Of-Charge-Voltage (EOCV). In [137] it was found that 90% of cycling losses resulted from the CV charging region. In [113], [121], [123], [126], [129] the effect of end-of-charge-voltage (EOCV), was investigated for LFP, LCO, and NCA chemistries. In these studies the EOCV ranged from 4.1V to 4.3V and all studies concluded that a higher EOCV lead to increased ageing. According to the authors of [123], a high cell voltage causes a higher potential in the cathode and a lower potential in the anode, which increases the electrolyte oxidation and reduction rates at the cathode and anode, respectively, resulting in surface film layer formation. Furthermore, in [126], a significant increase in degradation was found with an EOCV of 4.3V, compared to 4.1V and 4.2V, respectively. The results of [126] are shown in Figure 16. Based on a differential voltage analysis, the authors conclude that lithium plating is the cause of the increased degradation rate. At this very end of the charging process, the reduced diffusion capability of lithium into the graphite anode is said to cause lithium plating.

All of the above mentioned studies use different methods to model the degradation due the EOCV or EODV (End-Of-Discharge-Voltage). In [113], the authors develop an ageing model based on the addition of multiple single factor stress models. The total cycle life CL is calculated according to Eq.(**??**).

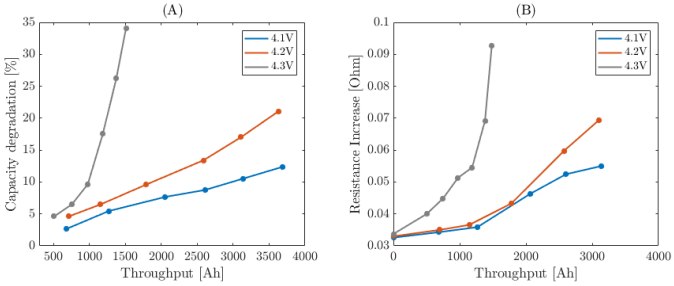

Fig. 16: Comparison of the capacity degradation (A) and resistance increase (B) of LCO cells tested at 1C, 25°C and various EOCV. significant increase in degradation is observed for the cells cycled up to 4.3V, and therefore too high EOCV should be avoided. Based on data obtained from [126]

.

$$CL = \frac{1}{SSF_0}\left(\frac{1}{SSF_T} + \frac{1}{SSF_{Id}} + \frac{1}{av_{EODV}^{-b}} + \frac{1}{SSF_{Ic}} + \frac{1}{cv_{EOCV}^{-d}}\right)$$

where:

- CL: total cycle life.
- SSF_x: Single stress factor model of x, where x = I_d, I_c; charge and discharge current rates.
- a, b, c, d: curve fit parameters

III-B6b Modelling Techniques: Average SoC

Other studies have investigated the effect of different starting or average SoC. In [73] three different average SoCs were investigated, 27.5%, 50% and 72.5%, all cycled with 35% DoD, 4C. Their results shown in Figure 17, show an increasing degradation rate for lower SoC, modelled as inversely exponentially dependent on SoC, as given in Eq.(24).

$$b(SoC) = 0.2943\exp(-0.01943SoC) \tag{24}$$

This increasing degradation rate at lower SoC can be explained by the fact that the impedance of the cell increases as the cell is discharged [21], [137], [142]. This results in reduced power capabilities and more self-heating. This is also temperature-dependent, and higher C-rates might aggravate its effect.

In [119] the effect of minimum SoC on various CS cycles for plug-in hybrid electric vehicles was tested on NMC-LMO cells at 30°C, 25-45% minimum SoC with varying C-rate. Their results show an exponentially increasing degradation at higher SoCs. Similar results are found in [94] for LFP cells cycled at 1-1.8C, 30°C. In both [94], [119] the calendar ageing was not subtracted, which might be a possible explanation for their results. In [112] a very slight increase in ageing was observed at higher SoC for cells cycled with a C-rate of 10C, whereas for lower temperatures and lower C-rates, the effect of SoC was found negligible. The authors followed an Arrhenius equation, where the degradation was linearly dependent on SoC, as shown in Eq.(25).

$$Q_{loss} = (\alpha SoC + \beta)\exp\frac{-E_a + \eta I}{R(273.15. + T)}Ah^z \tag{25}$$

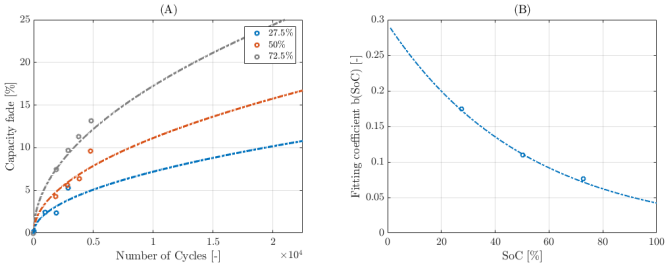

Fig. 17: (A): Ageing results for three different cells cycled with 35% DoD, 4C at 42.5°C around an average SoC of 27.5%, 50% and 72.5%. (B): Curve fitting coefficient $b(SoC)$ in eq.(24) for the three different ageing tests. Based on data obtained from [73].

The authors of [13] cycled NMC cells with various DoD at 1C, 35°C, and subtracted the expected calendar ageing results from their cycling ageing results. The resulting data showed the lowest ageing around an average SoC of 50%. Similar results were found in [84], [96].

III-B6c Modelling Limitations & Challenges: SoC (Cyclic)

Concerning the effect of EOCV, a consensus exists that a higher EOCV leads to increased degradation. However, at these high SoC levels, battery chargers charge with a decreasing average current to maintain a constant voltage instead of constant current charging in the majority of the SoC range. Therefore, the effect of EOCV might be attributed primarily to calendar ageing mechanisms.

Less consensus on the effect of average SoC on LIB ageing is observed. Partially due to the influence of other parameters such as temperature, DoD, C-rate, and chemistry. But also due to the other mechanical and kinetic changes inside the cell. Such as an increased impedance at lower SoC, and volume changes due to the different electrode intercalation compounds [143], [144], as shown in Figure 10. In [143], the authors analyzed five NCA cells each cycled with 20% DoD around evenly distributed SoC intervals. The highest degradation was observed for the cells cycled in stage 2 (see Figure 10).

A similar investigation was done in [47], where 10% DoD

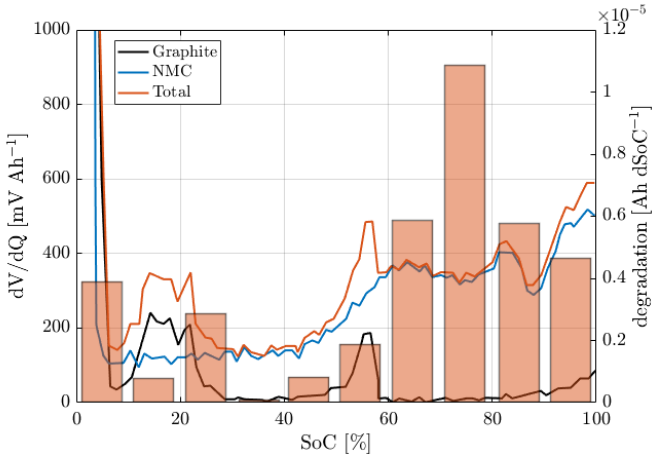

Fig. 18: (left): Differential voltage analysis of an NMC cell, and (right): the degradation rate of cycles with 10% DoD for 10 different SoC intervals. The orange bars illustrate the strong SoC dependency on the effect of DoD. The most degradation is observed at the place where the anode potential is the lowest or where there is a phase transition at the anode. These cells are cycled with 10% DoD, 1C, 45°C, around 10 different SoC regions. Based on data obtained from [47]

.

cycles are spread out evenly over the entire SoC range. The results are shown in Figure 18, and are in line with what was found in [143]. Here the bars show the total degradation per SoC range, whereas the lines show the DVA of both electrodes and the complete cell. However, the results of Figure 18 oppose their results for cells cycled with a DOD of 50%, which showed the least ageing with an average SoC 75%. This shows that SoC and DoD's effect have strong interdependencies that

are hard to capture in empirical ageing models, as the effect will always be different depending on the starting point and cycle depth. Aside from a high interdependence, testing for only a limited amount of time or cycles may also lead to false conclusions on total lifetime, as was demonstrated in [47]. Here, NMC cells were tested around 25-75% SoC with 1C at 20°C. In the first 300 full equivalent cycles (FEC), the most ageing was observed at the highest SoC. Nevertheless, the highest cycle lifetime was observed at the highest average SoC as well. Further investigation showed that a more stable SEI is formed at higher cell voltages, whereas the SEI formed at lower cell voltages evolves to be more porous. Especially the SEI formed in the CV region is said to better protect the anode material from the electrolyte. As a result, longer cycle life's were observed for higher cell voltages.

III-B6d Key Insights on SoC (Cyclic)

The following key insights can be summarized based on the above review:

- A higher EOCV results in increased ageing; due to the reduced current rate in the CV region, this is expected to be due to increased calendar ageing.
- The effect of SoC is strongly dependent on other operating conditions, such as C-rate, temperature and DoD. More specifically, cells tested at low C-rates, higher voltages, and higher temperatures are likely to have a significant calendar ageing superposition, resulting in less ageing at lower SoC. In contrast, cells cycled with higher C-rates or higher DoD appear to be more affected by the lower impedance at lower SoC. Probably having a higher cycle life when cycled around 50% SoC.
- A fast initial decrease in capacity due to high cell voltages does not necessarily have to result in a reduced lifetime, as higher cell voltages may lead to a more stable SEI layer.

7) Depth-of-Discharge

The final stress factor to be discussed is the DoD, sometimes also called cycle depth [6]. In this study, DoD is defined as the percentage of extracted charge with respect to the maximum available amount of charge. A usual rule of thumb is that an increasing DoD reduces the cycle lifetime [21], [79], [111]. However, as will be discussed, this is not valid for all reviewed studies. Generally, two different testing approaches exist to determine the detrimental effect of DoD: 1. starting from 100% SoC, or 2. cycling around a mean SoC. Both methods are limited because the starting point of the cycle determines the corresponding effect of DoD, as discussed in the previous section. Depending on the application of the model, one of the two methods can be preferred.

III-B7a Modelling Techniques: DoD

An often found correlation between DoD and degradation follows the Wöhler curve, also known as the S-N curve or Palmgren-Miner rule [146]. Originating from mechanical stress in railway-engineering, this curve describes an objects lifetime, expressed in terms of the number of cycles (N) and cyclic stress (S) [93]. For LIB degradation, it is frequently used to describe the battery cycle-life as a function of DoD. Here the degradation rate decreases as the DoD increases. Various papers have found good correlation with this dependency [46], [73], [79], [97], [98], [111], [122]. Some of their results are shown in Figures 19(a)-(b).

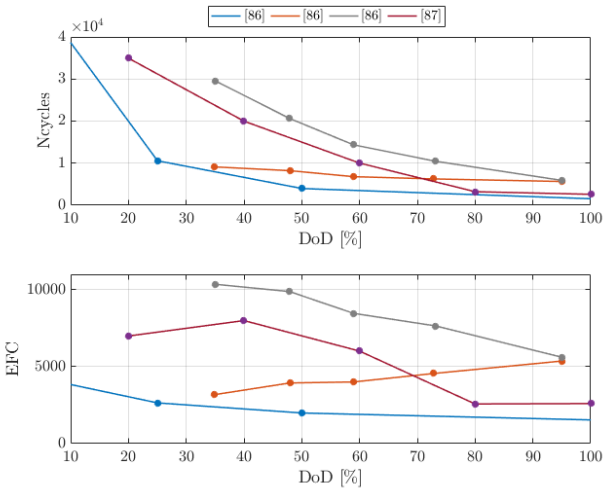

Fig. 19: Comparison of the effect of DoD in two different studies. Top figure: DoD versus cycles (a), and bottom figure versus full equivalent cycles (b). Even though many studies find a good correlation with the Wöhler curve in terms of number of cycles, in terms of total charge throughput cycle life does not necessarily decreases for higher DoD.

When plotted as a function of number of cycles, a good correlation with the Wöhler curve is observed. However, when plotted as a function of full equivalent cycles, this behaviour is not always seen. Therefore in terms of total charge throughput, cycle life does not necessarily have to decrease for a higher DoD.

Based on the Wöhler curve, several studies have modelled the degradation to be exponentially dependent on DoD [94], [97], [111], an example from [111] is shown in Eq.(26).

$$CL(DoD) = ae^{b \cdot DoD} + ce^{d \cdot DoD} \tag{26}$$

Here,

- $CL(DoD)$: cycle life as function of DoD
- a,b,c,d: curve fit parameters

Others, such as [73], have modelled the DoD dependency using a power law relationship as shown in Eq.(27)

$$C_{fade} = 0.0123 \cdot cd^{0.07162} \cdot nc^{0.5} \tag{27}$$

here,

- C_{fade}: percentage capacity fade
- cd: cycle depth / depth of discharge
- nc: number of cycles

III-B7b Modelling Limitations & Challenges: DoD

Even though the Wöhler curve has shown a good correlation with ageing data in several studies, readers and modellers

[6]Existing DoD definitions in the literature are contradictory, and at least four conflicting definitions are used, namely 1) the inverse of the SoC, 2) the energy discharged from the battery compared to 100% SoC, 3) the full cycle consisting of one equal discharging and charging event or 4) the half-cycle consisting of one charging or discharging event [145]

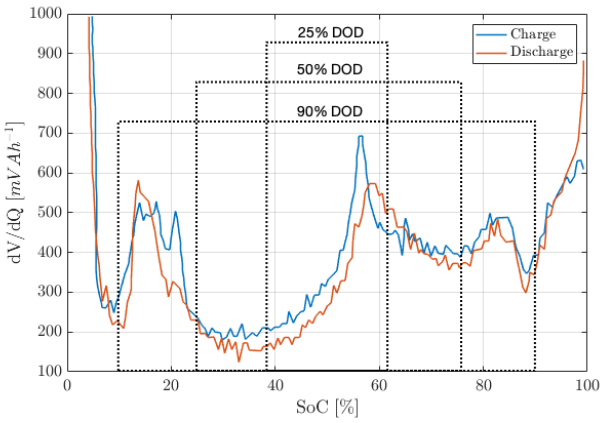

Fig. 20: Differential voltage curve for an NMC cell under slow charge and discharge rates. The number of phase transitions depends on the DoD and the starting SoC, as indicated by the different intervals.

should be aware that these results are also dependent on other stress factors and therefore cannot be generalized or extrapolated to other operating conditions.

In fact, in [47], [93], [143] it is argued that one of the causes of degradation due to DoD is the traversing between different phases of the anode and cathode. As a result, the effect of DoD is heavily SoC dependent. Following this analysis, for a given DoD it could be possible that the battery stays in the same voltage plateau, resulting in negligible effects between various DoD. Or a slight change in SoC might lead to a considerable capacity decrease (or resistance increase), as shown in Figures 18 and 20. Two observations are made: 1. The most degradation is observed at higher SoC, where the anode is in its second stage according to Figure 10 and the largest change in anode volume is observed [143]. 2. Secondly, regions where phase transitions occur lead to additional degradation. In [147] it was confirmed for an NMC cell that traversing of the voltage plateaus resulted in more volume changes of the cell, whereas the volume change is low if the cycle stays within a particular plateau region. These volume changes can cause particle cracking, resulting in an accelerated growth of the SEI layer [47], [148]. Therefore, the authors of [147] conclude that the stresses per full equivalent cycle are dependent on the number of voltage plateaus traversed.

Similar conclusions for NMC cells were drawn in [93], where an increased DoD showed an increased degradation. For all cases resulting in an almost linear course of degradation for both resistance and capacity. DVA showed that cycles that cross anode voltage plateaus caused additional degradation due to mechanical stress. Over time the voltage peaks decreased. The authors conclude that the disordering of the anode lattice could be a possible explanation. Another explanation could be an in-homogeneous load over the electrode, as was shown in simulation in [149], [150]. Overall the lowest degradation was observed for cells cycled around an average SoC of 50%, probably caused by a strong superposition of other SoC-dependent mechanisms caused by cell voltage or impedance.

A similar linear course of degradation was observed in [46], where the cycle life of batteries for satellite applications was investigated by cycling NCA cells with only 1-4 cycles per day. The authors noticed that as the cycling frequency increased, a linear component on top of $\sqrt{time}$ behaviour started to arise. This linear degradation of capacity and resistance increased as the DoD increased. Based on a destructive physical analysis, the authors argued that damage to the cathode's active material reduced lithium adsorption capability. Furthermore, Transmission Electron Microscopy showed that, compared to calendar ageing, the amorphous[7] layer was less thick and consisted of two layers of active material. A linear component as a result of cyclic ageing was observed in other studies as well [13], [46], [84], [111], [127]. An example of this is shown in Figure 12, where an increasing DoD results in an increasing linear degradation. Unfortunately, no further investigation on the root cause of DoD-dependent degradation was performed in [13], [46], [84], [111], [127].

Due to the complex correlations between SoC and DoD it is incredibly challenging to model their correlations. To this extend, none of the above described models can accurately model these effects outside the conditions at which these models are tested, which shows the importance of carefully selecting test conditions.

So far, all studies discussed have reported an increase in degradation for higher DOD, given that all other conditions are equal. However, in [47], [105] a higher DoD actually lead to less ageing. In [47] significantly less degradation was observed for cells cycled with 100% DoD compared to other DoDs, independent from C-rate and temperature. Using electrical impedance spectroscopy, the authors discovered that the resistance remained constant for a long time despite a fast initial increase. The cells cycled with a DoD of 50%, showed a more linear increase in resistance. As a result, it also reached the critical SEI layer resistance earlier, causing lithium plating and a reduced lifetime. Further investigation showed that the CV region played an important role in forming a stable SEI layer, indicating that its formation is strongly voltage-dependent and kinetically slow. Therefore, the cells cycled at 100% DoD might have a more stable SEI layer resulting in longer cycle life.

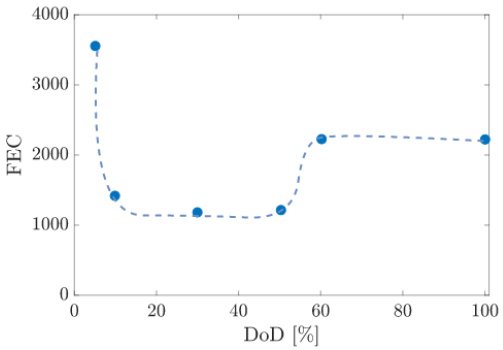

Fig. 21: Number of full equivalent cycles for different DOD ranges obtained in [105], before reaching 90% remaining capacity. Remarkably, less ageing is observed for high DoD cycles. The cells have been cycled with 1C at 30° around 50% average SoC.

[7]without a clearly defined shape or form

The effect of DOD on an LFP cell's cycle life was also tested in [105]. Their results are shown in Figure 21 and 22. The DoD-dependency on cycle life is shown in Figure 19(b), showing an increased cycle life for a DoD$\geq$50% around an average SoC of 50%, at 1C 30°C. In contrast to some of the studies mentioned above, the authors did not find any clear correlation between the anode staging phenomena and the DoD dependent degradation. Note, that these cells were tested at a starting SoC of 100%. Therefore, the reduced degradation at higher DoD's might result from a lower average cell voltage. Also, following the results of [47], it could be argued that a higher average voltage results in faster but more stable growth of the SEI layer. The total cycle life of these cells could therefore be improved on the long term. This is supported by the fact that only the cells cycled at 100% DoD showed an increase in degradation (both capacity and resistance) after 3000 FEC, possibly resulting from electrolyte depletion or lithium plating.

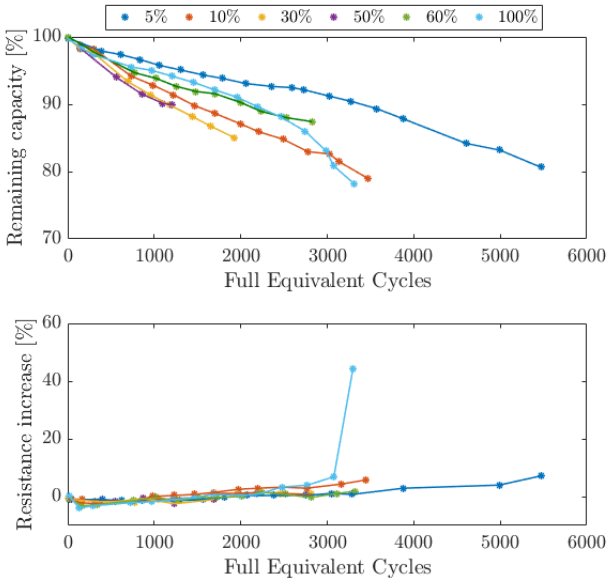

Fig. 22: Degradation of LFP cells cycled with varying DoD, 1C, 30°. The results show a reduced degradation for cells cycles with a DoD above 50% [105]. However, the increase in resistance for the cells cycled with 100% DoD around 3000 FEC could indicate the onset of lithium plating and therefore significantly reduce its lifetime.

Figure 22 also shows that the cells with a moderate increase in resistance only experienced low structural damage due to cycling [63]. Another possible explanation for the discrepancy in the results of [105], can be that the lattice structure of LFP cells better allows for complete delithiation compared to NMC cells, resulting from higher stability. [151], [152]. Furthermore, manganese-containing chemistries, such as the cells studied in [47], [93], [147], are more prone to SoC induced ageing. Due to ageing mechanisms such as Jahn-Teller distortion, transition metal dissolution, structural damage due to complete delithiation, and electrolyte oxidation [2], [21], [54]. Of course, additional testing and analysis should be carried out to pinpoint the exact cause of degradation.

III-B7c Key Insights on the effect of DoD

Based on the section above, the following key insights on the effect of DoD on LIB ageing can be summarized:

- Most often, the cycle life decreases as DoD increases. However, in terms of total charge throughput, different optima are observed at various DoD's.
- DoD effect can also be perceived differently due to the coexistence of various ageing mechanisms and the inter-dependency with other stress factors, such as high and low cell voltage, different temperatures, or various current rates. As a result, assessing DoD-dependent degradation can be very difficult, especially for highly varying power profiles.
- The effect of DoD is strongly SoC dependent. More specifically, the traversing of voltage plateaus, or the transitioning between electrode phases, has increased mechanical stress due to volume changes. Often resulting in a linear component in ageing behaviour. Additionally, the CV region can play a significant role in providing a stable SEI layer and therefore affect the degradation due to DoD.

IV. Current Challenges & Future Trends

This section provides an overview of the current challenges and future trends with respect to LIB ageing, and ageing modelling.

A. New Battery Chemistries

For EV and RES applications, two of the most common cathode materials are Lithium-Nickel-Manganese-Cobalt-Oxide (NMC) and Lithium-Iron-Phosphate (LFP) [153], with graphite as anode material. The main objective in the development of new chemistries is to improve performance. However, also the environmental and societal footprint of the raw materials will start to play a more significant role as the LIB market increases. Therefore the use of rare and toxic elements, such as Cobalt and Nickel, should be avoided as much as possible [153]–[155]. In the future, some promising new anode materials could be based on LTO, Silicon (Si) or Tin (Sn), or other carbon-based structures such as graphene or carbon nanotubes [154]. The list of future cathode materials is smaller, and will probably involve new combinations of the existing materials mentioned in section II, page 7 of this paper [155]. Another possible improvement could be the use of nanostructures. Besides incremental changes to existing technology, other more disruptive chemistries include Li-Air and Li-Sulfur, which achieve very high energy densities. Modelling the ageing behaviour of these new chemistries will play an important role in quantifying their performance. Si-C based anode materials for example, provide exceptional energy density at the expense of a significantly reduced lifetime due to structural damage [34]. For more information, interested readers are directed to [34], [154], [155].

B. Second-life Batteries

Besides new battery chemistries, another way to reduce the cost and environmental impact of LIBs is to use second-life batteries (SLB). SLBs are repurposed EV batteries deemed

unfit for EV applications but still have sufficient capacity for other stationary applications such as grid reinforcement. Reusing these batteries lowers the cost of LIBs while also lowering the environmental impact by reducing the demand for raw materials. In [156], [157], the authors showed that first-life battery performance is a critical parameter to assess the remaining value and state-of-health for second-life applications. As a result, modelling and optimizing battery ageing in both first- and second-life can reduce the environmental impact of LIBs. However, most of the studies currently only investigate ageing behaviour in the first part of LIB life. For example, studies that model the ageing behaviour as a function of $\sqrt{time}$ or $\sqrt{Ah}$, tend to miss out on ageing effects in the later part of their life, such as lithium plating, and are therefore less or not suitable for second-life applications.

C. Fast Charging

Range anxiety and long charging times are two of the main challenges for electric vehicles at this moment [158]. Fast charging is an effective tool for relieving EV users' range anxiety. Currently, most EVs can withstand maximum charging powers in the range of 50-150kW. However, new top-end vehicles, such as the Porsche Taycan or Audi e-tron GT, can charge with powers up to 350kW [159]. These maximum charging rates and total charging time are currently limited by the battery's rate capability and the thermal management of the EV. Naturally, charging at these high rates is far more damaging to the battery and to mitigate this, more and more EVs have thermally managed battery packs. Therefore, correlating the effects of temperature, C-rate, and DoD is important to accurately calculate the deteriorating effect of fast charging.

D. Thermally Managed Systems

Thermal management is becoming more common as a way to improve the lifetime of LIB systems. Thermal management for fast charging is an example of this. However, thermal management is also used at lower charging rates to prevent lithium plating at low temperatures. Other applications include stationary applications, such as RES integration or ancillary services. These systems generally have climate control systems, that control the temperature to be around 20-25°C to have optimal cycling performance. To this extend, extensive testing of ageing behaviour around room temperature could be argued to be vital for good modelling accuracy.

E. Artificial Intelligence for Ageing Estimation

As mentioned in the introduction, the different ageing estimation techniques such as PBMs, ECMs, or EMs all provide different trade-offs between modelling accuracy, complexity, and computational demand. Recently, various AI techniques have been investigated as ways to achieve high accuracy with low computational demand. These techniques can be differentiated into two groups. The first group train there AIs on model-fitted features, such as internal resistance and SoC, to estimate the SoH. These models then require other models to extract these internal parameters. The second group uses external features, such as open-circuit voltage and incremental capacity curves, to estimate SoH [20]. The latter do not rely on other models to calculate the internal parameters and therefore have a lower computational complexity, and as a result are better suited for real-time applications.

V. Conclusion

Due to their critical role in the electrification of transportation and the integration of renewable energy sources, lithium-ion batteries are recognized as a key technology in achieving the goals set in the Paris climate agreement. Understanding battery ageing is one of the main scientific problems related to LIBs and vital to understand better the trade-offs between characteristics such as performance, cost, and lifetime.

In this paper, a review on the behaviour and empirical modelling of LIB ageing was presented, focussing on the effect and interdependency of operational stress factors. The presented review concludes that it is very difficult to generalize ageing behaviour, with respect to the effect of operational conditions. Usually, the resulting ageing is caused by a combination of stress factors rather than attributable to a single stress factor. To this extent, users of empirical and semi-empirical battery ageing models should be cautious of their models' limitations and the correlations between the stress factors. To summarize some of the key findings:

- SEI growth is considered to be the most important ageing mechanism for both cycling and calendar ageing. A strong correlation with anode potential is observed during idle conditions: a higher SoC results in increased SEI layer growth. However, other kinetic effects during cycling can accelerate ageing at low SoC. SoC-dependent calendar ageing is often modelled to exponentially dependent, whereas its effect on cyclic ageing can have different forms depending on the operating conditions.
- Because of the passivation character of the SEI layer, the ageing behaviour is most commonly modelled using a t^z or Ah^z relationship, with $0.5 \leq z \leq 1$. Unfortunately, many cyclic ageing models do not differentiate between cyclic and calendar ageing, and therefore measure their combined effect. Others have subtracted calendar ageing from their cyclic ageing results to model the effect of cyclic ageing only, resulting in higher modelling accuracy.
- The Arrhenius law is an effective model for the temperature dependence of calendar ageing. However, during cycling, different ageing mechanisms are observed above and below room temperature. These should be considered when modelling cyclic ageing below room temperature. Since most studies are based on accelerated test conditions, this is frequently overlooked. Possible solutions include combining positive and negative activation energy in Arrhenius laws or including parabolic temperature dependencies.
- The effect of C-rate is often modelled to be exponentially dependent. Several studies, however, have found insignificant differences at C-rates less than 2. Furthermore, multiple studies have found a strong correlation between C-rate and temperature; as temperature rises, the impact of C-rate decreases significantly. Many models do not take this

into account, which is in part due to accelerated testing conditions.

- Several studies modelled the DoD dependent degradation based on Wohler curves or other exponential curves. However, the effect of DoD is directly related to other SoC associated mechanisms and is therefore probably the most difficult stress factor to model. Additionally, the impact of DoD is affected by volume change due to electrode phase transitions and is thus also related to C-rate and temperature.

The summation of conclusions are all examples of the challenges involved in modelling LIB ageing behaviour. Readers and modellers can mitigate these challenges by improving the design of ageing tests, ageing models, and ageing model applications using the knowledge provided in this paper. The authors hope that by doing so, they can help with overcoming the challenges of LIBs.

REFERENCES

[1] B. L. Ellis, K. T. Lee, and L. F. Nazar, "Positive electrode materials for li-ion and li-batteries," *Chemistry of Materials*, vol. 22, no. 3, pp. 691–714, 2010. [Online]. Available: https://doi.org/10.1021/cm902696j

[2] X. Han, L. Lu, Y. Zheng, X. Feng, Z. Li, J. Li, and M. Ouyang, "A review on the key issues of the lithium ion battery degradation among the whole life cycle," *eTransportation*, vol. 1, p. 100005, 2019. [Online]. Available: https://www.sciencedirect.com/science/article/pii/S2590116819300050

[3] I. Tsiropoulos, D. Tarvydas, and N. Lebedeva, "Li-ion batteries for mobility and stationary applications7," Joint Research Centre (European Commission), Tech. Rep., 2018.

[4] Y. Zheng, M. Ouyang, L. Lu, J. Li, X. Han, L. Xu, H. Ma, T. A. Dollmeyer, and V. Freyermuth, "Cell state-of-charge inconsistency estimation for lifepo4 battery pack in hybrid electric vehicles using mean-difference model," *Applied Energy*, vol. 111, pp. 571–580, 2013. [Online]. Available: https://www.sciencedirect.com/science/article/pii/S0306261913004601

[5] M. Doyle, T. F. Fuller, and J. Newman, "Modeling of galvanostatic charge and discharge of the lithium/polymer/insertion cell," vol. 140, no. 6, pp. 1526–1533, jun 1993. [Online]. Available: https://doi.org/10.1149/1.2221597

[6] M. Jafari, K. Khan, and L. Gauchia, "Deterministic models of li-ion battery aging: It is a matter of scale," *Journal of Energy Storage*, vol. 20, pp. 67 – 77, 2018. [Online]. Available: http://www.sciencedirect.com/science/article/pii/S2352152X18303098

[7] P. W. C. Northrop, M. Pathak, D. Rife, S. De, S. Santhanagopalan, and V. R. Subramanian, "Efficient simulation and model reformulation of two-dimensional electrochemical thermal behavior of lithium-ion batteries," vol. 162, no. 6, pp. A940–A951, 2015. [Online]. Available: https://doi.org/10.1149/2.0341506jes

[8] R. Darling and J. Newman, "Modeling side reactions in composite li y mn2 o 4 electrodes," vol. 145, no. 3, pp. 990–998, mar 1998. [Online]. Available: https://doi.org/10.1149/1.1838376

[9] P. Ramadass, B. Haran, P. M. Gomadam, R. White, and B. N. Popov, "Development of first principles capacity fade model for li-ion cells," vol. 151, no. 2, p. A196, 2004. [Online]. Available: https://doi.org/10.1149/1.1634273

[10] J. Christensen and J. Newman, "A mathematical model for the lithium-ion negative electrode solid electrolyte interphase," vol. 151, no. 11, p. A1977, 2004. [Online]. Available: https://doi.org/10.1149/1.1804812

[11] A. V. Randall, R. D. Perkins, X. Zhang, and G. L. Plett, "Controls oriented reduced order modeling of solid-electrolyte interphase layer growth," *Journal of Power Sources*, vol. 209, pp. 282–288, 2012. [Online]. Available: https://www.sciencedirect.com/science/article/pii/S0378775312005368

[12] A. Barré, B. Deguilhem, S. Grolleau, M. Gérard, F. Suard, and D. Riu, "A review on lithium-ion battery ageing mechanisms and estimations for automotive applications," *Journal of Power Sources*, vol. 241, pp. 680–689, 2013. [Online]. Available: https://www.sciencedirect.com/science/article/pii/S0378775313008185

[13] J. Schmalstieg, S. Käbitz, M. Ecker, and D. U. Sauer, "A holistic aging model for li(nimnco)o2 based 18650 lithium-ion batteries," *Journal of Power Sources*, vol. 257, pp. 325–334, 2014. [Online]. Available: https://www.sciencedirect.com/science/article/pii/S0378775314001876

[14] S. Nejad, D. Gladwin, and D. Stone, "A systematic review of lumped-parameter equivalent circuit models for real-time estimation of lithium-ion battery states," *Journal of Power Sources*, vol. 316, pp. 183–196, 2016. [Online]. Available: https://www.sciencedirect.com/science/article/pii/S0378775316302427

[15] Z. Wang, J. Ma, and L. Zhang, "State-of-health estimation for lithium-ion batteries based on the multi-island genetic algorithm and the gaussian process regression," *IEEE Access*, vol. 5, pp. 21 286–21 295, 2017.

[16] M. Berecibar, F. Devriendt, M. Dubarry, I. Villarreal, N. Omar, W. Verbeke, and J. Van Mierlo, "Online state of health estimation on nmc cells based on predictive analytics," *Journal of Power Sources*, vol. 320, pp. 239–250, 2016. [Online]. Available: https://www.sciencedirect.com/science/article/pii/S0378775316304827

[17] H. Pan, Z. Lü, H. Wang, H. Wei, and L. Chen, "Novel battery state-of-health online estimation method using multiple health indicators and an extreme learning machine," *Energy*, vol. 160, pp. 466–477, 2018. [Online]. Available: https://www.sciencedirect.com/science/article/pii/S0360544218312854

[18] D. Yang, Y. Wang, R. Pan, R. Chen, and Z. Chen, "State-of-health estimation for the lithium-ion battery based on support vector regression," *Applied Energy*, vol. 227, pp. 273–283, 2018, transformative Innovations for a Sustainable Future – Part III. [Online]. Available: https://www.sciencedirect.com/science/article/pii/S0306261917311169

[19] K. Liu, X. Hu, Z. Wei, Y. Li, and Y. Jiang, "Modified gaussian process regression models for cyclic capacity prediction of lithium-ion batteries," *IEEE Transactions on Transportation Electrification*, vol. 5, no. 4, pp. 1225–1236, 2019.

[20] Y. Li, K. Liu, A. M. Foley, A. Zülke, M. Berecibar, E. Nanini-Maury, J. Van Mierlo, and H. E. Hoster, "Data-driven health estimation and lifetime prediction of lithium-ion batteries: A review," *Renewable and Sustainable Energy Reviews*, vol. 113, p. 109254, 2019. [Online]. Available: https://www.sciencedirect.com/science/article/pii/S136403211930454X

[21] J. Vetter, P. Novák, M. Wagner, C. Veit, K.-C. Möller, J. Besenhard, M. Winter, M. Wohlfahrt-Mehrens, C. Vogler, and A. Hammouche, "Ageing mechanisms in lithium-ion batteries," *Journal of Power Sources*, vol. 147, no. 1, pp. 269–281, 2005. [Online]. Available: https://www.sciencedirect.com/science/article/pii/S0378775305000832

[22] M. Broussely, P. Biensan, F. Bonhomme, P. Blanchard, S. Herreyre, K. Nechev, and R. Staniewicz, "Main aging mechanisms in li ion batteries," *Journal of Power Sources*, vol. 146, no. 1, pp. 90 – 96, 2005, selected papers pressented at the 12th International Meeting on Lithium Batteries. [Online]. Available: http://www.sciencedirect.com/science/article/pii/S0378775305005082

[23] X. Han, L. Lu, Y. Zheng, X. Feng, Z. Li, J. Li, and M. Ouyang, "A review on the key issues of the lithium ion battery degradation among the whole life cycle," *eTransportation*, vol. 1, p. 100005, 2019. [Online]. Available: http://www.sciencedirect.com/science/article/pii/S2590116819300050

[24] X. Han, M. Ouyang, L. Lu, L. Jianqiu, Y. Zheng, and Z. Li, "A comparative study of commercial lithium ion battery cycle life in electrical vehicle: Aging mechanism identification," *Journal of Power Sources*, vol. 251, p. 38–54, 04 2014.

[25] M. Scarfogliero, S. Carmeli, F. Castelli-Dezza, M. Mauri, M. Rossi, G. Marchegiani, and E. Rovelli, "Lithium-ion batteries for electric vehicles: A review on aging models for vehicle-to-grid services," in *2018 International Conference of Electrical and Electronic Technologies for Automotive*, 2018, pp. 1–6.

[26] A. Ahmadian, M. Sedghi, A. Elkamel, M. Fowler, and M. Aliakbar Golkar, "Plug-in electric vehicle batteries degradation modeling for smart grid studies: Review, assessment and conceptual framework," *Renewable and Sustainable Energy Reviews*, vol. 81, pp. 2609 – 2624, 2018. [Online]. Available: http://www.sciencedirect.com/science/article/pii/S1364032117310067

[27] J. R. Xiong, L. Li, "Towards a smarter battery management system: A critical review on battery state of health monitoring methods," *Journal of Power Sources*, vol. 405, pp. 18–29, 2018.

[28] M. Berecibar, I. Gandiaga, I. Villarreal, N. Omar, J. Van Mierlo, and P. Van den Bossche, "Critical review of state of health estimation methods of li-ion batteries for real applications," *Renewable and Sustainable Energy Reviews*, vol. 56, pp. 572 – 587, 2016.

[Online]. Available: http://www.sciencedirect.com/science/article/pii/S1364032115013076

[29] M. Lucu, E. Martinez-Laserna, I. Gandiaga, and H. Camblong, "A critical review on self-adaptive li-ion battery ageing models," *Journal of Power Sources*, vol. 401, pp. 85 – 101, 2018. [Online]. Available: http://www.sciencedirect.com/science/article/pii/S0378775318309297

[30] M. H. Lipu, M. Hannan, A. Hussain, M. Hoque, P. J. Ker, M. Saad, and A. Ayob, "A review of state of health and remaining useful life estimation methods for lithium-ion battery in electric vehicles: Challenges and recommendations," *Journal of Cleaner Production*, vol. 205, pp. 115 – 133, 2018. [Online]. Available: http://www.sciencedirect.com/science/article/pii/S0959652618327793

[31] J. Vetter, P. Novák, M. Wagner, C. Veit, K.-C. Möller, J. Besenhard, M. Winter, M. Wohlfahrt-Mehrens, C. Vogler, and A. Hammouche, "Ageing mechanisms in lithium-ion batteries," *Journal of Power Sources*, vol. 147, no. 1, pp. 269 – 281, 2005. [Online]. Available: http://www.sciencedirect.com/science/article/pii/S0378775305000832

[32] C. R. Birkl, M. R. Roberts, E. McTurk, P. G. Bruce, and D. A. Howey, "Degradation diagnostics for lithium ion cells," *Journal of Power Sources*, vol. 341, pp. 373–386, 2017. [Online]. Available: https://www.sciencedirect.com/science/article/pii/S0378775316316998

[33] A. Barré, B. Deguilhem, S. Grolleau, M. Gérard, F. Suard, and D. Riu, "A review on lithium-ion battery ageing mechanisms and estimations for automotive applications," *Journal of Power Sources*, vol. 241, pp. 680–689, 2013. [Online]. Available: https://www.sciencedirect.com/science/article/pii/S0378775313008185

[34] K. Kalaga, M.-T. F. Rodrigues, S. E. Trask, I. A. Shkrob, and D. P. Abraham, "Calendar-life versus cycle-life aging of lithium-ion cells with silicon-graphite composite electrodes," *Electrochimica Acta*, vol. 280, pp. 221–228, 2018. [Online]. Available: https://www.sciencedirect.com/science/article/pii/S0013468618311344

[35] C. Pastor-Fernández, T. F. Yu, W. D. Widanage, and J. Marco, "Critical review of non-invasive diagnosis techniques for quantification of degradation modes in lithium-ion batteries," *Renewable and Sustainable Energy Reviews*, vol. 109, pp. 138–159, 2019. [Online]. Available: https://www.sciencedirect.com/science/article/pii/S136403211930200X

[36] E. Sarasketa-Zabala, F. Aguesse, I. Villarreal, L. Rodríguez-Martínez, C. López, and P. Kubiak, "Understanding lithium inventory loss and sudden performance fade in cylindrical cells during cycling with deep-discharge steps," *The Journal of Physical Chemistry C*, vol. 119, pp. 896–906, 01 2015.

[37] C. Pastor-Fernández, T. F. Yu, W. D. Widanage, and J. Marco, "Critical review of non-invasive diagnosis techniques for quantification of degradation modes in lithium-ion batteries," *Renewable and Sustainable Energy Reviews*, vol. 109, pp. 138–159, 2019. [Online]. Available: https://www.sciencedirect.com/science/article/pii/S136403211930200X

[38] C. Delacourt and M. Safari, *Mathematical Modeling of Aging of Li-Ion Batteries*. London: Springer London, 2016, pp. 151–190. [Online]. Available: https://doi.org/10.1007/978-1-4471-5677-2_5

[39] P. Keil, S. F. Schuster, J. Wilhelm, J. Travi, A. Hauser, R. C. Karl, and A. Jossen, "Calendar aging of lithium-ion batteries," *Journal of The Electrochemical Society*, vol. 163, no. 9, pp. A1872–A1880, 2016. [Online]. Available: https://doi.org/10.1149/2.0411609jes

[40] P. Arora, R. E. White, and M. Doyle, "Capacity fade mechanisms and side reactions in lithium-ion batteries," *Journal of The Electrochemical Society*, vol. 145, no. 10, pp. 3647–3667, oct 1998. [Online]. Available: https://doi.org/10.1149/1.1838857

[41] J. Park, W. A. Appiah, S. Byun, D. Jin, M.-H. Ryou, and Y. M. Lee, "Semi-empirical long-term cycle life model coupled with an electrolyte depletion function for large-format graphite/lifepo4 lithium-ion batteries," *Journal of Power Sources*, vol. 365, pp. 257–265, 2017. [Online]. Available: https://www.sciencedirect.com/science/article/pii/S0378775317311278

[42] B. Xu, A. Oudalov, A. Ulbig, G. Andersson, and D. S. Kirschen, "Modeling of lithium-ion battery degradation for cell life assessment," *IEEE Transactions on Smart Grid*, vol. 9, no. 2, pp. 1131–1140, 2018.

[43] X. Han, M. Ouyang, L. Lu, J. Li, Y. Zheng, and Z. Li, "A comparative study of commercial lithium ion battery cycle life in electrical vehicle: Aging mechanism identification," *Journal of Power Sources*, vol. 251, pp. 38–54, 2014. [Online]. Available: https://www.sciencedirect.com/science/article/pii/S0378775313018569

[44] B. Scrosati and J. Garche, "Lithium batteries: Status, prospects and future," *Journal of Power Sources*, vol. 195, no. 9, pp. 2419–2430, 2010. [Online]. Available: https://www.sciencedirect.com/science/article/pii/S0378775309020564

[45] E. Peled, D. Bar Tow, A. Merson, A. Gladkich, L. Burstein, and D. Golodnitsky, "Composition, depth profiles and lateral distribution of materials in the sei built on hopg-tof sims and xps studies," *Journal of Power Sources*, vol. 97-98, pp. 52–57, 2001, proceedings of the 10th International Meeting on Lithium Batteries. [Online]. Available: https://www.sciencedirect.com/science/article/pii/S0378775301005055

[46] J. Hall, T. Lin, G. Brown, P. Biensan, and F. Bonhomme, "Decay processes and life predictions for lithium ion satellite cells," 06 2006.

[47] A. Maheshwari, "Modelling, aging and optimal operation of lithium-ion batteries," Ph.D. dissertation, Department of Electrical Engineering, Oct. 2018, proefschrift.

[48] N. Lin, Z. Jia, Z. Wang, H. Zhao, G. Ai, X. Song, Y. Bai, V. Battaglia, C. Sun, J. Qiao, K. Wu, and G. Liu, "Understanding the crack formation of graphite particles in cycled commercial lithium-ion batteries by focused ion beam - scanning electron microscopy," *Journal of Power Sources*, vol. 365, pp. 235–239, 2017. [Online]. Available: https://www.sciencedirect.com/science/article/pii/S0378775317310698

[49] M. Koltypin, Y. S. Cohen, B. Markovsky, Y. Cohen, and D. Aurbach, "The study of lithium insertion–deinsertion processes into composite graphite electrodes by in situ atomic force microscopy (afm)," *Electrochemistry Communications*, vol. 4, no. 1, pp. 17–23, 2002. [Online]. Available: https://www.sciencedirect.com/science/article/pii/S1388248101002648

[50] H. Ekstrom. Electrode balancing of a lithium-ion battery with comsol. [Online]. Available: https://www.comsol.com/blogs/electrode-balancing-of-a-lithium-ion-battery-with-comsol/

[51] M. Broussely, P. Biensan, F. Bonhomme, P. Blanchard, S. Herreyre, K. Nechev, and R. Staniewicz, "Main aging mechanisms in li ion batteries," *Journal of Power Sources*, vol. 146, no. 1, pp. 90–96, 2005, selected papers pressented at the 12th International Meeting on Lithium Batteries. [Online]. Available: https://www.sciencedirect.com/science/article/pii/S0378775305005082

[52] H. J. Ploehn, P. Ramadass, and R. E. White, "Solvent diffusion model for aging of lithium-ion battery cells," *Journal of The Electrochemical Society*, vol. 151, no. 3, p. A456, 2004. [Online]. Available: https://doi.org/10.1149/1.1644601

[53] M. Ecker, J. B. Gerschler, J. Vogel, S. Käbitz, F. Hust, P. Dechent, and D. U. Sauer, "Development of a lifetime prediction model for lithium-ion batteries based on extended accelerated aging test data," *Journal of Power Sources*, vol. 215, pp. 248–257, 2012. [Online]. Available: https://www.sciencedirect.com/science/article/pii/S0378775312008671

[54] M. Wohlfahrt-Mehrens, C. Vogler, and J. Garche, "Aging mechanisms of lithium cathode materials," *Journal of Power Sources*, vol. 127, no. 1, pp. 58–64, 2004, eighth Ulmer Electrochemische Tage. [Online]. Available: https://www.sciencedirect.com/science/article/pii/S0378775303009376

[55] X. Liao, Q. Huang, S. Mai, X. Wang, M. Xu, L. Xing, Y. Liao, and W. Li, "Understanding self-discharge mechanism of layered nickel cobalt manganese oxide at high potential," *Journal of Power Sources*, vol. 286, pp. 551–556, 2015. [Online]. Available: https://www.sciencedirect.com/science/article/pii/S0378775315006710

[56] T. Joshi, K. Eom, G. Yushin, and T. F. Fuller, "Effects of dissolved transition metals on the electrochemical performance and SEI growth in lithium-ion batteries," *Journal of The Electrochemical Society*, vol. 161, no. 12, pp. A1915–A1921, 2014. [Online]. Available: https://doi.org/10.1149/2.0861412jes

[57] W. Li, "Review—an unpredictable hazard in lithium-ion batteries from transition metal ions: Dissolution from cathodes, deposition on anodes and elimination strategies," *Journal of The Electrochemical Society*, vol. 167, no. 9, p. 090514, apr 2020. [Online]. Available: https://doi.org/10.1149/1945-7111/ab847f

[58] T.-F. Yi, L.-J. Jiang, J. Shu, C.-B. Yue, R.-S. Zhu, and H.-B. Qiao, "Recent development and application of li4ti5o12 as anode material of lithium ion battery," *Journal of Physics and Chemistry of Solids*, vol. 71, no. 9, pp. 1236–1242, 2010. [Online]. Available: https://www.sciencedirect.com/science/article/pii/S0022369710001526

[59] W. Lu, J. Liu, Y. Sun, and K. Amine, "Electrochemical performance of li4/3ti5/3o4/li1+x(ni1/3co1/3mn1/3)1xo2 cell for high power applications," *Journal of Power Sources*, vol. 167, no. 1, pp. 212–216, 2007. [Online]. Available: https://www.sciencedirect.com/science/article/pii/S0378775307000985

[60] B. Priyono, P. W. Winowatan, A. Z. Syahrial, Faizah, and A. Subhan, "Optimizing the performance of li4ti5o12/LTO by addition of silicon microparticle in half cell litium-ion battery anode," *IOP Conference Series: Earth and Environmental Science*, vol. 105, p. 012121, jan 2018. [Online]. Available: https://doi.org/10.1088/1755-1315/105/1/012121

[61] C. Zhan, T. Wu, J. Lu, and K. Amine, "Dissolution, migration, and deposition of transition metal ions in li-ion batteries exemplified by mn-based cathodes – a critical review," *Energy Environ. Sci.*, vol. 11, pp. 243–257, 2018. [Online]. Available: http://dx.doi.org/10.1039/C7EE03122J

[62] S. Bourlot, P. Blanchard, and S. Robert, "Investigation of aging mechanisms of high power li-ion cells used for hybrid electric vehicles," *Journal of Power Sources*, vol. 196, no. 16, pp. 6841–6846, 2011, 15th International Meeting on Lithium Batteries (IMLB). [Online]. Available: https://www.sciencedirect.com/science/article/pii/S0378775310017106

[63] M. Kassem, J. Bernard, R. Revel, S. Pélissier, F. Duclaud, and C. Delacourt, "Calendar aging of a graphite/lifepo4 cell," *Journal of Power Sources*, vol. 208, pp. 296–305, 2012. [Online]. Available: https://www.sciencedirect.com/science/article/pii/S0378775312004284

[64] K. Edström, T. Gustafsson, and J. Thomas, "The cathode–electrolyte interface in the li-ion battery," *Electrochimica Acta*, vol. 50, no. 2, pp. 397–403, 2004, polymer Batteries and Fuel Cells:Selection of Papers from First International Conference. [Online]. Available: https://www.sciencedirect.com/science/article/pii/S0013468604006486

[65] K. Amine, J. Liu, I. Belharouak, S.-H. Kang, I. Bloom, D. Vissers, and G. Henriksen, "Advanced cathode materials for high-power applications," *Journal of Power Sources*, vol. 146, no. 1, pp. 111–115, 2005, selected papers pressented at the 12th International Meeting on Lithium Batteries. [Online]. Available: https://www.sciencedirect.com/science/article/pii/S0378775305005173

[66] D. Aurbach, K. Gamolsky, B. Markovsky, G. Salitra, Y. Gofer, U. Heider, R. Oesten, and M. Schmidt, "The study of surface phenomena related to electrochemical lithium intercalation into li[sub x]MO[sub y] host materials (m = ni, mn)," *Journal of The Electrochemical Society*, vol. 147, no. 4, p. 1322, 2000. [Online]. Available: https://doi.org/10.1149/1.1393357

[67] C. Love, A. Korovina, C. Patridge, K. Swider-Lyons, M. Twigg, and D. Ramaker, "Review of lifepo4 phase transition mechanisms and new observations from x-ray absorption spectroscopy," *Journal of the Electrochemical Society*, vol. 160, pp. A3153–A3161, 01 2013.

[68] K. Y. Chung and K.-B. Kim, "Investigations into capacity fading as a result of a jahn–teller distortion in 4v limn2o4 thin film electrodes," *Electrochimica Acta*, vol. 49, no. 20, pp. 3327–3337, 2004. [Online]. Available: https://www.sciencedirect.com/science/article/pii/S0013468604002865

[69] X. Li, Y. Xu, and C. Wang, "Suppression of jahn–teller distortion of spinel limn2o4 cathode," *Journal of Alloys and Compounds*, vol. 479, no. 1, pp. 310–313, 2009. [Online]. Available: https://www.sciencedirect.com/science/article/pii/S0925838808022391

[70] M. Lewerenz, J. Münnix, J. Schmalstieg, S. Käbitz, M. Knips, and D. U. Sauer, "Systematic aging of commercial lifepo4—graphite cylindrical cells including a theory explaining rise of capacity during aging," *Journal of Power Sources*, vol. 345, pp. 254–263, 2017. [Online]. Available: https://www.sciencedirect.com/science/article/pii/S037877531730143X

[71] M. Lewerenz, G. Fuchs, L. Becker, and D. U. Sauer, "Irreversible calendar aging and quantification of the reversible capacity loss caused by anode overhang," *Journal of Energy Storage*, vol. 18, pp. 149–159, 2018. [Online]. Available: https://www.sciencedirect.com/science/article/pii/S2352152X18301191

[72] E. Redondo-Iglesias, P. Venet, and S. Pelissier, "Eyring acceleration model for predicting calendar ageing of lithium-ion batteries," *Journal of Energy Storage*, vol. 13, pp. 176–183, 2017. [Online]. Available: https://www.sciencedirect.com/science/article/pii/S2352152X17300634

[73] D. Stroe, "Lifetime models for lithium-ion batteries used in virtual power plant applications," Ph.D. dissertation, Nov. 2014.

[74] S. Grolleau, A. Delaille, H. Gualous, P. Gyan, R. Revel, J. Bernard, E. Redondo-Iglesias, and J. Peter, "Calendar aging of commercial graphite/lifepo4 cell – predicting capacity fade under time dependent storage conditions," *Journal of Power Sources*, vol. 255, pp. 450–458, 2014. [Online]. Available: https://www.sciencedirect.com/science/article/pii/S0378775313019411

[75] E. Sarasketa-Zabala, I. Gandiaga, L. Rodriguez-Martinez, and I. Villarreal, "Calendar ageing analysis of a lifepo4/graphite cell with dynamic model validations: Towards realistic lifetime predictions," *Journal of Power Sources*, vol. 272, pp. 45–57, 2014. [Online]. Available: https://www.sciencedirect.com/science/article/pii/S0378775314013068

[76] Y. Zheng, Y.-B. He, K. Qian, B. Li, X. Wang, J. Li, C. Miao, and F. Kang, "Effects of state of charge on the degradation of lifepo4/graphite batteries during accelerated storage test," *Journal of Alloys and Compounds*, vol. 639, pp. 406–414, 2015. [Online]. Available: https://www.sciencedirect.com/science/article/pii/S0925838815008944

[77] D. Stroe, M. Swierczynski, S. K. Kær, and R. Teodorescu, "Degradation behavior of lithium-ion batteries during calendar ageing—the case of the internal resistance increase," *IEEE Transactions on Industry Applications*, vol. 54, no. 1, pp. 517–525, 2018.

[78] I. Bloom, B. Cole, J. Sohn, S. Jones, E. Polzin, V. Battaglia, G. Henriksen, C. Motloch, R. Richardson, T. Unkelhaeuser, D. Ingersoll, and H. Case, "An accelerated calendar and cycle life study of li-ion cells," *Journal of Power Sources*, vol. 101, no. 2, pp. 238–247, 2001. [Online]. Available: https://www.sciencedirect.com/science/article/pii/S0378775301007832

[79] M. Swierczynski, D. Stroe, A. Stan, R. Teodorescu, and S. K. Kær, "Lifetime estimation of the nanophosphate $LiFePO_4$/C battery chemistry used in fully electric vehicles," *IEEE Transactions on Industry Applications*, vol. 51, no. 4, pp. 3453–3461, 2015.

[80] A. Eddahech, O. Briat, and J.-M. Vinassa, "Performance comparison of four lithium–ion battery technologies under calendar aging," *Energy*, vol. 84, pp. 542–550, 2015. [Online]. Available: https://www.sciencedirect.com/science/article/pii/S0360544215003138

[81] P. Röder, B. Stiaszny, J. C. Ziegler, N. Baba, P. Lagaly, and H.-D. Wiemhöfer, "The impact of calendar aging on the thermal stability of a limn2o4–li(ni1/3mn1/3co1/3)o2/graphite lithium-ion cell," *Journal of Power Sources*, vol. 268, pp. 315–325, 2014. [Online]. Available: https://www.sciencedirect.com/science/article/pii/S0378775314008945

[82] J. Belt, V. Utgikar, and I. Bloom, "Calendar and phev cycle life aging of high-energy, lithium-ion cells containing blended spinel and layered-oxide cathodes," *Journal of Power Sources*, vol. 196, no. 23, pp. 10 213–10 221, 2011. [Online]. Available: https://www.sciencedirect.com/science/article/pii/S0378775311016107

[83] Julius, A. Maheshwari, M. Heck, S. Lux, and M. Vetter, "Impedance change and capacity fade of lithium nickel manganese cobalt oxide-based batteries during calendar aging," *Journal of Power Sources*, vol. 353, pp. 183–194, 2017. [Online]. Available: https://www.sciencedirect.com/science/article/pii/S037877531730397X

[84] J. de Hoog, J.-M. Timmermans, D. Ioan-Stroe, M. Swierczynski, J. Jaguemont, S. Goutam, N. Omar, J. Van Mierlo, and P. Van Den Bossche, "Combined cycling and calendar capacity fade modeling of a nickel-manganese-cobalt oxide cell with real-life profile validation," *Applied Energy*, vol. 200, pp. 47–61, 2017. [Online]. Available: https://www.sciencedirect.com/science/article/pii/S0306261917305251

[85] J. Wang, J. Purewal, P. Liu, J. Hicks-Garner, S. Soukazian, E. Sherman, A. Sorenson, L. Vu, H. Tataria, and M. Verbrugge, "Degradation of lithium ion batteries employing graphite negatives and nickel-cobalt-manganese oxide + spinel manganese oxide positives: Part 1, aging mechanisms and life estimation," *Journal of Power Sources*, vol. 269, 11 2014.

[86] I. Baghdadi, O. Briat, J.-Y. Delétage, P. Gyan, and J.-M. Vinassa, "Lithium battery aging model based on dakin's degradation approach," *Journal of Power Sources*, vol. 325, pp. 273–285, 2016. [Online]. Available: https://www.sciencedirect.com/science/article/pii/S0378775316307388

[87] E. Thomas, I. Bloom, J. Christophersen, and V. Battaglia, "Statistical methodology for predicting the life of lithium-ion cells via accelerated degradation testing," *Journal of Power Sources*, vol. 184, no. 1, pp. 312–317, 2008. [Online]. Available: https://www.sciencedirect.com/science/article/pii/S0378775308012032

[88] E. Redondo-Iglesias, P. Venet, and S. Pélissier, "Influence of the non-conservation of soc value during calendar ageing tests on modelling the capacity loss of batteries," in *2015 Tenth International Conference on Ecological Vehicles and Renewable Energies (EVER)*, 2015, pp. 1–5.

[89] H. YOSHIDA, N. IMAMURA, T. INOUE, K. TAKEDA, and H. NAITO, "Verification of life estimation model for space lithium-ion cells," *Electrochemistry*, vol. 78, no. 5, pp. 482–488, 2010.

[90] S. Buller, "Impedance based simulation models for energy storage devices in advanced automotive power systems," Ph.D. dissertation, Aachen, 2003, zugl.: Aachen, Techn. Hochsch., Diss., 2002. [Online]. Available: https://publications.rwth-aachen.de/record/58812

[91] D. Andre, M. Meiler, K. Steiner, H. Walz, T. Soczka-Guth, and D. Sauer, "Characterization of high-power lithium-ion batteries by electrochemical impedance spectroscopy. ii: Modelling," *Journal of Power Sources*, vol. 196, pp. 5349–5356, 06 2011.

[92] S. Käbitz, J. B. Gerschler, M. Ecker, Y. Yurdagel, B. Emmermacher, D. André, T. Mitsch, and D. U. Sauer, "Cycle and calendar life study of a graphite—lini1/3mn1/3co1/3o2 li-ion high energy system. part

a: Full cell characterization," *Journal of Power Sources*, vol. 239, pp. 572–583, 2013. [Online]. Available: https://www.sciencedirect.com/science/article/pii/S0378775313004369

[93] M. Ecker, N. Nieto, S. Käbitz, J. Schmalstieg, H. Blanke, A. Warnecke, and D. U. Sauer, "Calendar and cycle life study of li(nimnco)o2-based 18650 lithium-ion batteries," *Journal of Power Sources*, vol. 248, pp. 839–851, 2014. [Online]. Available: https://www.sciencedirect.com/science/article/pii/S0378775313016510

[94] L. Lam and P. Bauer, "Practical capacity fading model for li-ion battery cells in electric vehicles," *IEEE Transactions on Power Electronics*, vol. 28, no. 12, pp. 5910–5918, 2013.

[95] M. Reichert, D. Andre, A. Rösmann, P. Janssen, H.-G. Bremes, D. Sauer, S. Passerini, and M. Winter, "Influence of relaxation time on the lifetime of commercial lithium-ion cells," *Journal of Power Sources*, vol. 239, pp. 45–53, 2013. [Online]. Available: https://www.sciencedirect.com/science/article/pii/S0378775313004448

[96] M. Ecker, J. B. Gerschler, J. Vogel, S. Käbitz, F. Hust, P. Dechent, and D. U. Sauer, "Development of a lifetime prediction model for lithium-ion batteries based on extended accelerated aging test data," *Journal of Power Sources*, vol. 215, pp. 248–257, 2012. [Online]. Available: https://www.sciencedirect.com/science/article/pii/S0378775312008671

[97] A. Millner, "Modeling lithium ion battery degradation in electric vehicles," in *2010 IEEE Conference on Innovative Technologies for an Efficient and Reliable Electricity Supply*, 2010, pp. 349–356.

[98] C. Guenther, B. Schott, W. Hennings, P. Waldowski, and M. A. Danzer, "Model-based investigation of electric vehicle battery aging by means of vehicle-to-grid scenario simulations," *Journal of Power Sources*, vol. 239, pp. 604–610, 2013. [Online]. Available: https://www.sciencedirect.com/science/article/pii/S0378775313003066

[99] R. Wright, C. Motloch, J. Belt, J. Christophersen, C. Ho, R. Richardson, I. Bloom, S. Jones, V. Battaglia, G. Henriksen, T. Unkelhaeuser, D. Ingersoll, H. Case, S. Rogers, and R. Sutula, "Calendar- and cycle-life studies of advanced technology development program generation 1 lithium-ion batteries," *Journal of Power Sources*, vol. 110, no. 2, pp. 445–470, 2002. [Online]. Available: https://www.sciencedirect.com/science/article/pii/S0378775302002100

[100] S. K. Rechkemmer, X. Zang, W. Zhang, and O. Sawodny, "Empirical li-ion aging model derived from single particle model," *Journal of Energy Storage*, vol. 21, pp. 773–786, 2019. [Online]. Available: https://www.sciencedirect.com/science/article/pii/S2352152X18307588

[101] M. Petit, E. Prada, and V. Sauvant-Moynot, "Development of an empirical aging model for li-ion batteries and application to assess the impact of vehicle-to-grid strategies on battery lifetime," *Applied Energy*, vol. 172, pp. 398–407, 2016. [Online]. Available: https://www.sciencedirect.com/science/article/pii/S0306261916304500

[102] V. A. Sethuraman, L. J. Hardwick, V. Srinivasan, and R. Kostecki, "Surface structural disordering in graphite upon lithium intercalation/deintercalation," *Journal of Power Sources*, vol. 195, no. 11, pp. 3655–3660, 2010. [Online]. Available: https://www.sciencedirect.com/science/article/pii/S0378775309022964

[103] W.-S. Yoon, K. Y. Chung, J. McBreen, and X.-Q. Yang, "A comparative study on structural changes of lico1/3ni1/3mn1/3o2 and lini0.8co0.15al0.05o2 during first charge using in situ xrd," *Electrochemistry Communications*, vol. 8, no. 8, pp. 1257–1262, 2006. [Online]. Available: https://www.sciencedirect.com/science/article/pii/S138824810600227X

[104] D. Manka and E. Ivers-Tiffée, "Electro-optical measurements of lithium intercalation/de-intercalation at graphite anode surfaces." *Electrochimica Acta*, vol. 186, pp. 642–653, 2015. [Online]. Available: https://www.sciencedirect.com/science/article/pii/S0013468615306538

[105] E. Sarasketa-Zabala, I. Gandiaga, E. Martinez-Laserna, L. Rodriguez-Martinez, and I. Villarreal, "Cycle ageing analysis of a lifepo4/graphite cell with dynamic model validations: Towards realistic lifetime predictions," *Journal of Power Sources*, vol. 275, pp. 573–587, 2015. [Online]. Available: https://www.sciencedirect.com/science/article/pii/S0378775314017728

[106] A. Marongiu, M. Roscher, and D. U. Sauer, "Influence of the vehicle-to-grid strategy on the aging behavior of lithium battery electric vehicles," *Applied Energy*, vol. 137, pp. 899–912, 2015. [Online]. Available: https://www.sciencedirect.com/science/article/pii/S030626191400645X

[107] R. Dufo-López and J. L. Bernal-Agustín, "Multi-objective design of pv–wind–diesel–hydrogen–battery systems," *Renewable Energy*, vol. 33, no. 12, pp. 2559–2572, 2008. [Online]. Available: https://www.sciencedirect.com/science/article/pii/S0960148108000724

[108] S. Mishra, M. Pecht, T. Smith, I. McNee, and R. Harris, "Remaining life prediction of electronic products using life consumption monitoring approach," 01 2002.

[109] Y.-L. Lee and T. Tjhung, "Chapter 3 - rainflow cycle counting techniques," in *Metal Fatigue Analysis Handbook*, Y.-L. Lee, M. E. Barkey, and H.-T. Kang, Eds. Boston: Butterworth-Heinemann, 2012, pp. 89–114. [Online]. Available: https://www.sciencedirect.com/science/article/pii/B9780123852045000033

[110] J. Wang, P. Liu, J. Hicks-Garner, E. Sherman, S. Soukiazian, M. Verbrugge, H. Tataria, J. Musser, and P. Finamore, "Cycle-life model for graphite-lifepo4 cells," *Journal of Power Sources*, vol. 196, no. 8, pp. 3942–3948, 2011. [Online]. Available: https://www.sciencedirect.com/science/article/pii/S0378775310021269

[111] N. Omar, M. Abdel Monem, Y. Firouz, J. Salminen, J. Smekens, O. Hegazy, H. Gualous, G. Mulder, P. Van den Bossche, T. Coosemans, and J. Van Mierlo, "Lithium iron phosphate based battery – assessment of the aging parameters and development of cycle life model," *Applied Energy*, vol. 113, pp. 1575–1585, 01 2014.

[112] G. Suri and S. Onori, "A control-oriented cycle-life model for hybrid electric vehicle lithium-ion batteries," *Energy*, vol. 96, pp. 644–653, 2016. [Online]. Available: https://www.sciencedirect.com/science/article/pii/S0360544215016382

[113] Z. Li, L. Lu, M. Ouyang, and Y. Xiao, "Modeling the capacity degradation of lifepo4/graphite batteries based on stress coupling analysis," *Journal of Power Sources*, vol. 196, pp. 9757–9766, 11 2011.

[114] F. Todeschini, S. Onori, and G. Rizzoni, "An experimentally validated capacity degradation model for li-ion batteries in phevs applications," *IFAC Proceedings Volumes*, vol. 45, no. 20, pp. 456–461, 2012, 8th IFAC Symposium on Fault Detection, Supervision and Safety of Technical Processes. [Online]. Available: https://www.sciencedirect.com/science/article/pii/S1474667016347966

[115] M. L. Bacci, F. Cheli, E. Sabbioni, D. Tarsitano, and M. Vignati, "Aging models for high capacity lifepo4 cells," in *2017 International Conference of Electrical and Electronic Technologies for Automotive*, 2017, pp. 1–6.

[116] M. Ebrahimi, M. Rastegar, M. Mohammadi, A. Palomino, and M. Parvania, "Stochastic charging optimization of v2g-capable pevs: A comprehensive model for battery aging and customer service quality," *IEEE Transactions on Transportation Electrification*, vol. 6, no. 3, pp. 1026–1034, 2020.

[117] M. Schimpe, M. E. von Kuepach, M. Naumann, H. C. Hesse, K. Smith, and A. Jossen, "Comprehensive modeling of temperature-dependent degradation mechanisms in lithium iron phosphate batteries," *Journal of The Electrochemical Society*, vol. 165, no. 2, pp. A181–A193, 2018. [Online]. Available: https://doi.org/10.1149/2.1181714jes

[118] M. Ouyang, X. Feng, X. Han, L. Lu, Z. Li, and X. He, "A dynamic capacity degradation model and its applications considering varying load for a large format li-ion battery," *Applied Energy*, vol. 165, pp. 48–59, 2016. [Online]. Available: https://www.sciencedirect.com/science/article/pii/S0306261915016360

[119] A. Cordoba-Arenas, S. Onori, Y. Guezennec, and G. Rizzoni, "Capacity and power fade cycle-life model for plug-in hybrid electric vehicle lithium-ion battery cells containing blended spinel and layered-oxide positive electrodes," *Journal of Power Sources*, vol. 278, pp. 473–483, 2015. [Online]. Available: https://www.sciencedirect.com/science/article/pii/S0378775314020758

[120] M. Mauri, F. Castelli-Dezza, M. S. Carmeli, M. Scarforgliero, and G. Marchegiani, "Electro-thermal aging model of li -ion batteries for vehicle-to-grid services," in *2019 AEIT International Conference of Electrical and Electronic Technologies for Automotive (AEIT AUTOMOTIVE)*, 2019, pp. 1–6.

[121] A. Hoke, A. Brissette, K. Smith, A. Pratt, and D. Maksimovic, "Accounting for lithium-ion battery degradation in electric vehicle charging optimization," *IEEE Journal of Emerging and Selected Topics in Power Electronics*, vol. 2, no. 3, pp. 691–700, 2014.

[122] K. Smith, M. Earleywine, E. Wood, J. Neubauer, and A. Pesaran, "Comparison of plug-in hybrid electric vehicle battery life across geographies and drive-cycles," vol. 1, 6 2012. [Online]. Available: https://www.osti.gov/biblio/1044471

[123] L. Su, J. Zhang, C. Wang, Y. Zhang, Z. Li, Y. Song, T. Jin, and Z. Ma, "Identifying main factors of capacity fading in lithium ion cells using orthogonal design of experiments," *Applied Energy*, vol. 163, pp. 201–210, 2016. [Online]. Available: https://www.sciencedirect.com/science/article/pii/S0306261915014555

[124] V. Sangwan, R. Kumar, and A. K. Rathore, "An empirical capacity degradation modeling and prognostics of remaining useful life of li-ion battery using unscented kalman filter," in *2018 8th IEEE India*

International Conference on Power Electronics (IICPE), 2018, pp. 1–6.

[125] H. Dai, X. Zhang, W. Gu, X. Wei, and Z. Sun, "A semi-empirical capacity degradation model of ev li-ion batteries based on eyring equation," in *2013 IEEE Vehicle Power and Propulsion Conference (VPPC)*, 2013, pp. 1–5.

[126] Y. Gao, J. Jiang, C. Zhang, W. Zhang, Z. Ma, and Y. Jiang, "Lithium-ion battery aging mechanisms and life model under different charging stresses," *Journal of Power Sources*, vol. 356, pp. 103–114, 2017. [Online]. Available: https://www.sciencedirect.com/science/article/pii/S0378775317305876

[127] Y. Cui, C. Du, G. Yin, Y. Gao, L. Zhang, T. Guan, L. Yang, and F. Wang, "Multi-stress factor model for cycle lifetime prediction of lithium ion batteries with shallow-depth discharge," *Journal of Power Sources*, vol. 279, pp. 123–132, 2015, 9th International Conference on Lead-Acid Batteries – LABAT 2014. [Online]. Available: https://www.sciencedirect.com/science/article/pii/S037877531500004X

[128] J. Guo, Z. Li, and M. Pecht, "A bayesian approach for li-ion battery capacity fade modeling and cycles to failure prognostics," *Journal of Power Sources*, vol. 281, pp. 173–184, 2015. [Online]. Available: https://www.sciencedirect.com/science/article/pii/S0378775315001925

[129] S. S. Choi and H. S. Lim, "Factors that affect cycle-life and possible degradation mechanisms of a li-ion cell based on licoo2," *Journal of Power Sources*, vol. 111, no. 1, pp. 130–136, 2002. [Online]. Available: https://www.sciencedirect.com/science/article/pii/S0378775302003051

[130] B. Ratnakumar, M. Smart, L. Whitcanack, and R. Ewell, "The impedance characteristics of mars exploration rover li-ion batteries," *Journal of Power Sources*, vol. 159, pp. 1428–1439, 09 2006.

[131] C. Huang, J. Sakamoto, J. Wolfenstine, and S. Surampudi, "The limits of low-temperature performance of li-ion cells," *Journal of The Electrochemical Society*, vol. 147, pp. 2893–2896, 08 2000.

[132] S. Zhang, K. Xu, and R. Jow, "060. the low temperature performance of li-ion batteries," *Journal of Power Sources*, vol. 115, pp. 137–140, 03 2003.

[133] T. Waldmann, M. Wilka, M. Kasper, M. Fleischhammer, and M. Wohlfahrt-Mehrens, "Temperature dependent ageing mechanisms in lithium-ion batteries – a post-mortem study," *Journal of Power Sources*, vol. 262, pp. 129–135, 2014. [Online]. Available: https://www.sciencedirect.com/science/article/pii/S0378775314004352

[134] M. Bauer, C. Guenther, M. Kasper, M. Petzl, and M. A. Danzer, "Discrimination of degradation processes in lithium-ion cells based on the sensitivity of aging indicators towards capacity loss," *Journal of Power Sources*, vol. 283, pp. 494–504, 2015. [Online]. Available: https://www.sciencedirect.com/science/article/pii/S0378775315003766

[135] H. p. Lin, D. Chua, M. Salomon, H.-C. Shiao, M. Hendrickson, E. Plichta, and S. Slane, "Low-temperature behavior of li-ion cells," *Electrochemical and Solid-State Letters*, vol. 4, no. 6, p. A71, 2001. [Online]. Available: https://doi.org/10.1149/1.1368736

[136] A. Eddahech, O. Briat, and J.-M. Vinassa, "Performance comparison of four lithium–ion battery technologies under calendar aging," *Energy*, vol. 84, pp. 542–550, 2015. [Online]. Available: https://www.sciencedirect.com/science/article/pii/S0360544215003138

[137] G. Ning, B. Haran, and B. N. Popov, "Capacity fade study of lithium-ion batteries cycled at high discharge rates," *Journal of Power Sources*, vol. 117, no. 1, pp. 160–169, 2003. [Online]. Available: https://www.sciencedirect.com/science/article/pii/S0378775303000296

[138] S. S. Zhang, "The effect of the charging protocol on the cycle life of a li-ion battery," *Journal of Power Sources*, vol. 161, no. 2, pp. 1385–1391, 2006. [Online]. Available: https://www.sciencedirect.com/science/article/pii/S0378775306011839

[139] K. Jalkanen, J. Karppinen, L. Skogström, T. Laurila, M. Nisula, and K. Vuorilehto, "Cycle aging of commercial nmc/graphite pouch cells at different temperatures," *Applied Energy*, vol. 154, pp. 160–172, 2015. [Online]. Available: https://www.sciencedirect.com/science/article/pii/S0306261915005735

[140] S. F. Schuster, T. Bach, E. Fleder, J. Müller, M. Brand, G. Sextl, and A. Jossen, "Nonlinear aging characteristics of lithium-ion cells under different operational conditions," *Journal of Energy Storage*, vol. 1, pp. 44–53, 2015. [Online]. Available: https://www.sciencedirect.com/science/article/pii/S2352152X15000092

[141] P. Niehoff, E. Kraemer, and M. Winter, "Parametrisation of the influence of different cycling conditions on the capacity fade and the internal resistance increase for lithium nickel manganese cobalt oxide/graphite cells," *Journal of Electroanalytical Chemistry*, vol. 707, pp. 110–116, 2013. [Online]. Available: https://www.sciencedirect.com/science/article/pii/S1572665713003925

[142] T. Borsche, A. Ulbig, M. Koller, and G. Andersson, "Power and energy capacity requirements of storages providing frequency control reserves," in *2013 IEEE Power Energy Society General Meeting*, 2013, pp. 1–5.

[143] S. Gantenbein, M. Schönleber, M. Weiss, and E. Ivers-Tiffée, "Capacity fade in lithium-ion batteries and cyclic aging over various state-of-charge ranges," *Sustainability*, vol. 11, no. 23, 2019. [Online]. Available: https://www.mdpi.com/2071-1050/11/23/6697

[144] M. P. Mercer, M. Otero, M. Ferrer-Huerta, A. Sigal, D. E. Barraco, H. E. Hoster, and E. P. Leiva, "Transitions of lithium occupation in graphite: A physically informed model in the dilute lithium occupation limit supported by electrochemical and thermodynamic measurements," *Electrochimica Acta*, vol. 324, p. 134774, 2019. [Online]. Available: https://www.sciencedirect.com/science/article/pii/S0013468619316457

[145] M. Koller, T. Borsche, A. Ulbig, and G. Andersson, "Defining a degradation cost function for optimal control of a battery energy storage system," in *2013 IEEE Grenoble Conference*, 2013, pp. 1–6.

[146] A. Ahmadian, M. Sedghi, A. Elkamel, M. Fowler, and M. Aliakbar Golkar, "Plug-in electric vehicle batteries degradation modeling for smart grid studies: Review, assessment and conceptual framework," *Renewable and Sustainable Energy Reviews*, vol. 81, pp. 2609–2624, 2018. [Online]. Available: https://www.sciencedirect.com/science/article/pii/S1364032117310067

[147] K.-Y. Oh, J. B. Siegel, L. Secondo, S. U. Kim, N. A. Samad, J. Qin, D. Anderson, K. Garikipati, A. Knobloch, B. I. Epureanu, C. W. Monroe, and A. Stefanopoulou, "Rate dependence of swelling in lithium-ion cells," *Journal of Power Sources*, vol. 267, pp. 197–202, 2014. [Online]. Available: https://www.sciencedirect.com/science/article/pii/S0378775314007228

[148] J. Dahn, "Phase diagram of lixc6," *Physical Review B*, vol. 44, no. 17, pp. 9170–9177, 1991, cited By 669. [Online]. Available: https://www.scopus.com/inward/record.uri?eid=2-s2.0-0000846309&doi=10.1103%2fPhysRevB.44.9170&partnerID=40&md5=e777836b078d70d65c9ef02252f94a8b

[149] T. Fuller, M. Doyle, and J. Newman, "Simulation and optimization of the dual lithium ion insertion cell," *Journal of the Electrochemical Society*, vol. 141, no. 1, pp. 1–10, 1994, cited By 1080. [Online]. Available: https://www.scopus.com/inward/record.uri?eid=2-s2.0-0028320402&doi=10.1149%2f1.2054684&partnerID=40&md5=20ed1c34676320d56974bbc245545c61

[150] M. Doyle, T. Fuller, and J. Newman, "Modeling of galvanostatic charge and discharge of the lithium/ polymer/insertion cell," *Journal of the Electrochemical Society*, vol. 140, no. 6, pp. 1526–1533, 1993, cited By 1901. [Online]. Available: https://www.scopus.com/inward/record.uri?eid=2-s2.0-0027608142&doi=10.1149%2f1.2221597&partnerID=40&md5=d536c68caf41d4f2a4507caece3e4adf

[151] W.-J. Zhang, "Structure and performance of lifepo4 cathode materials: A review," *Journal of Power Sources*, vol. 196, no. 6, pp. 2962–2970, 2011. [Online]. Available: https://www.sciencedirect.com/science/article/pii/S037877531002104X

[152] C. Masquelier, S. Patoux, C. Wurm, and M. Morcrette, "Polyanion-based positive electrode materials," 01 2003.

[153] X. Shu, Y. Guo, W. Yang, K. Wei, and G. Zhu, "Life-cycle assessment of the environmental impact of the batteries used in pure electric passenger cars," *Energy Reports*, vol. 7, pp. 2302–2315, 2021. [Online]. Available: https://www.sciencedirect.com/science/article/pii/S2352484721002547

[154] D. Deng, "Li-ion batteries: basics, progress, and challenges," *Energy Science & Engineering*, vol. 3, no. 5, pp. 385–418. [Online]. Available: https://onlinelibrary.wiley.com/doi/abs/10.1002/ese3.95

[155] V. Etacheri, R. Marom, R. Elazari, G. Salitra, and D. Aurbach, "Challenges in the development of advanced li-ion batteries: a review," *Energy Environ. Sci.*, vol. 4, pp. 3243–3262, 2011. [Online]. Available: http://dx.doi.org/10.1039/C1EE01598B

[156] E. Martinez-Laserna, E. Sarasketa-Zabala, I. Villarreal Sarria, D.-I. Stroe, M. Swierczynski, A. Warnecke, J.-M. Timmermans, S. Goutam, N. Omar, and P. Rodriguez, "Technical viability of battery second life: A study from the ageing perspective," *IEEE Transactions on Industry Applications*, vol. 54, no. 3, pp. 2703–2713, 2018.

[157] E. W. J. Neubauer, K. Smith and A. Pesaran, "Identifying and overcoming critical barriers to widespread second use of pev batteries," National Renewable Energy Laboratory, Tech. Rep., 2015.

[158] I. Aghabali, J. Bauman, P. J. Kollmeyer, Y. Wang, B. Bilgin, and A. Emadi, "800-v electric vehicle powertrains: Review and analysis of benefits, challenges, and future trends," *IEEE Transactions on Transportation Electrification*, vol. 7, no. 3, pp. 927–948, 2021.

[159] FASTNED, "Fastned - vehicles and charging tips," https://support.fastned.nl/hc/en-gb/sections/115000180588-Vehicles-charging-tips?page=1#articles, 2021.

Wiljan Vermeer received the bachelor's degree in Electrical Engineering from the Eindhoven University of Technology, Eindhoven, the Netherlands, in 2016 and the master's degree in Electrical Engineering from Delft University of Technology, Delft, the Netherlands, in 2018. Since 2018, he has been working toward the Ph.D. degree in the field of solar-powered smart charging systems at Delft University of Technology, Delft, The Netherlands. His research interests include EV smart charging, battery degradation, and DC-DC power electronic converters for smart charging.

Gautham Ram Chandra Mouli Dr.ir. Gautham Ram (M'14) is an assistant professor in the DC systems, Energy conversion and Storage group in the Department of Electrical Sustainable Energy at the Delft University of Technology, The Netherlands. He received his bachelor's and master's in Electrical Engineering from the National Institute of Technology Trichy, India in 2011 and the Delft University of Technology in 2013, respectively. He received his PhD from the Delft University in 2018 for the development of a solar powered V2G electric vehicle charger compatible with CHAdeMO, CCS/COMBO and designed smart charging algorithms (with PRE, ABB and UT Austin). It was awarded the 'Most significant innovation in electric vehicles' award from IDtechEx in 2018 and the 'Best Tech Idea of 2018'by KIJK. From 2017 to 2019, he was a postdoctoral research at TU Delft pursuing his research on power converters for EV charging, smart charging of EVs, trolley busses.

Gautham Ram was awarded the best paper prize in the IEEE Transactions on Industrial Informatics in 2018, the Best Poster prize at Erasmus Energy Forum 2016, Netherlands and the Best Paper prize at the IEEE INDICON Conference 2009, India. He is involved in many projects with industrial and academic partners at national and EU level concerning electric mobility and renewable energy such as PV charging of electric vehicles, OSCD, Trolley 2.0, Flexgrid, Flexinet and NEON. His current research focusses on electric vehicles charging, PV systems, power electronics and intelligent control. He is the coordinator and a lecturer for Massive Open Online Course (MOOC) on Electric cars on edX.org with 175,000 learners from 175 countries. He is the Vice-chair of IEEE Industrial Electronic Society Benelux chapter.

Pavol Bauer received the master's degree in electrical engineering from the Technical University of Kosice, Košice, Slovakia in 1985, and the Ph.D. degree from the Delft University of Technology, Delft, The Netherlands, in 1995. He is currently a Full Professor with the Department of Electrical Sustainable Energy, Delft University of Technology, the Head of DC Systems, Energy Conversion and Storage Group, a Professor with the Brno University of Technology, Brno, Czechia, and a Honorary Professor with Politehnica University Timi¸soara, Timi¸soara, Romania. From 2002 to 2003, he was with KEMA (DNV GL, Arnhem) on different projects related to power electronics applications in power systems. He has authored and coauthored more than 120 journal and 500 conference papers in his field with H factor Google scholar 40, Web of Science 26, he is the author or coauthor of eight books, holds seven international patents and organized several tutorials at the international conferences. He has worked on many projects for industry concerning wind and wave energy, power electronic applications for power systems such as Smarttrafo, HVDC systems, projects for smart cities such as PV charging of electric vehicles, PV and storage integration, contactless charging, and participated in several Leonardo da Vinci, H2020 and Electric Mobility Europe EU projects as a Project Partner (ELINA, INETELE, E-Pragmatic, Micact, Trolley 2.0, OSCD, P2P, Progressus) and a Coordinator (PEMCWebLab.com-Edipe, SustEner, Eranet DCMICRO). His main research focuses on power electronics for charging of electric vehicles and dc grids. He is the Former Chairman of Benelux IEEE Joint Industry Applications Society, Power Electronics and Power Engineering Society chapter, the Chairman of the Power Electronics and Motion Control council, Member of the Executive Committee of European Power Electronics Association and the International Steering Committee at numerous conferences.